International Geology Review
Publication details, including instructions for authors and subscription information:
http://www.informaworld.com/smpp/title~content=t902953900

Step-over in the structure controlling the regional west tilt of the Sierra Nevada microplate: eastern escarpment system to Kern Canyon system

J. Saleeby [a]; Z. Saleeby [a]; E. Nadin [a]; G. Maheo [bcd]
[a] Division of Geological and Planetary Sciences, California Institute of Technology, Pasadena, CA, USA [b] Université de Lyon, Lyon, France [c] Université Lyon 1, Villeurbanne, France [d] Laboratoire de Sciences de la Terre, ENS, Lyon CNRS, Villeurbanne, France

Online Publication Date: 01 July 2009

To cite this Article Saleeby, J., Saleeby, Z., Nadin, E. and Maheo, G.(2009)'Step-over in the structure controlling the regional west tilt of the Sierra Nevada microplate: eastern escarpment system to Kern Canyon system',International Geology Review,51:7,634 — 669

To link to this Article: DOI: 10.1080/00206810902867773

URL: http://dx.doi.org/10.1080/00206810902867773

International Geology Review
Vol. 51, Nos. 7–8, July–August 2009, 634–669

Step-over in the structure controlling the regional west tilt of the Sierra Nevada microplate: eastern escarpment system to Kern Canyon system

J. Saleeby[a]*, Z. Saleeby[a], E. Nadin[a] and G. Maheo[bcd]

[a]*Division of Geological and Planetary Sciences, California Institute of Technology, Pasadena, CA 91125, USA;* [b]*Université de Lyon, Lyon F-69622, France;* [c]*Université Lyon 1, Villeurbanne F-69622, France;* [d]*Laboratoire de Sciences de la Terre, ENS, Lyon CNRS, UMR 5570, Bat Géode, 2 Rue Dubois, Villeurbanne 69622, France*

(*Accepted 27 February 2009*)

The Sierra Nevada and Great Valley are coupled, and behave as a semi-rigid microplate. The microplate formed as it was calved off the western edge of the Nevadaplano in the late Miocene, at which time westward regional tilting began. Tilting is controlled by west-side-up normal faulting primarily along the eastern Sierra escarpment system. Uplift and exhumation along the eastern Sierra are balanced by subsidence and sedimentation along the western Great Valley. The west tilt of the microplate is expressed by the west slope of a regional relict landscape surface that developed across much of the Sierra Nevada basement, and by the westward continuation of the surface as the basal Eocene nonconformity of the west-dipping Great Valley Tertiary section. The rigid behaviour of the microplate breaks down along its southern ~100–150 km segment as expressed by seismicity, pervasive faulting and the development of a deep marine basin, the San Joaquin Basin (SJB), whose facies and palaeogeographic patterns diverge from regional patterns of the rest of the Great Valley. The disrupted state of the southern segment of the microplate resulted from its Late Cretaceous position above a regional lateral ramp in the underlying Franciscan-related subduction megathrust. The Kern Canyon fault system began its polyphase history as a complex oblique dextral shear zone above the megathrust lateral ramp. It was remobilized in the Neogene as an oblique transfer structure partitioning differential extension between the southern Sierra Nevada and the SJB. In Quaternary time, the Kern Canyon zone was again remobilized as a west-side-up normal fault system whose geomorphic and structural expressions are best developed south of ~36.4° N. This normal fault system controls the west tilt of the relict landscape surface in the southern Sierra region, as well as the west dip pattern in the strata of the adjacent SJB. To the east of the Kern Canyon normal fault system, the relict landscape surface slopes continuously southwards from the high eastern Sierra into a low-lying, multiply extended terrane. Thus, from ~36.4° N southwards, the west tilt along the western Sierra and the west dip of the adjacent Great Valley strata are controlled by the Kern Canyon system. Fresh normal scarps along the eastern Sierra escarpment system become more subdued and ultimately die out southwards from ~36.4° N. Thus, currently, the controlling structure for the west tilt of the microplate steps westwards in the south from the eastern escarpment system over to the Kern Canyon system.

Keywords: microplate; remobilization; delamination; epeirogeny

*Email: jason@gps.caltech.edu

ISSN 0020-6814 print/ISSN 1938-2839 online

DOI: 10.1080/00206810902867773
http://www.informaworld.com

Introduction

The Sierra Nevada constitutes part of a semi-rigid crustal block that, along with the coupled Great Valley, has been termed the Sierra Nevada microplate (Argus and Gordon 1991; Dixon *et al.* 2000; Sella *et al.* 2002). This 'microplate' is bounded to the west by the San Andreas transpressive plate juncture and to the east by the eastern Sierra escarpment system (Figure 1), which also forms the western boundary of the Basin and Range extensional province. The Sierra Nevada may be characterized to a first order as a westward-tilted fault block whose tilting and related basement exhumation are balanced by subsidence and sedimentation in the Great Valley (Unruh 1991). The west tilt of the microplate is well documented by low west dips of Tertiary cover strata lying along the western Sierra–Great Valley transition, and is further expressed in the Great Valley subsurface by the west slope of the basement surface that reaches ~8 km depth along the synclinal axis of the Valley (Wentworth *et al.* 1995). The controlling structures for the regional west tilt of the microplate for the most part correspond to west-side-up normal faults of the eastern escarpment system, most prominent along the western margin

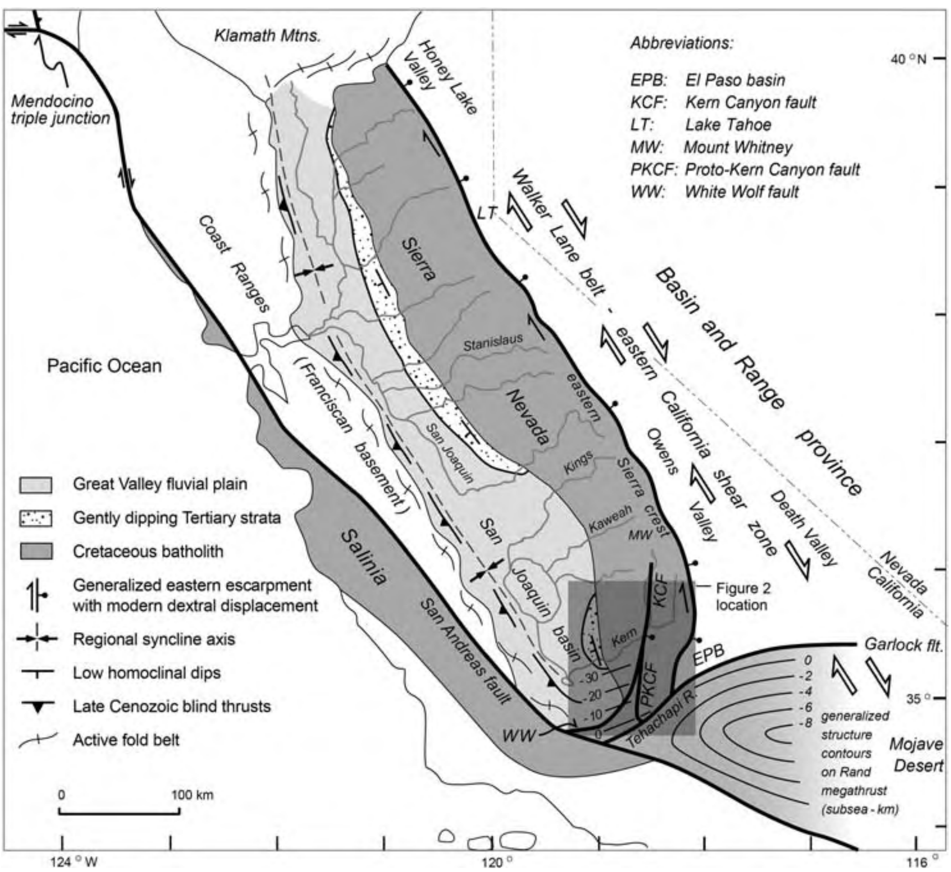

Figure 1. Index map of the central California region showing the Sierra Nevada microplate, its major river drainages, its bounding structural systems consisting of the eastern escarpment, Garlock fault, San Andreas transpressive zone and northern convergence zone with the Klamath Mountains province, and other tectonic features discussed in the text. Sources are referenced in the text.

of Owens Valley. Currently, the Owens Valley escarpment system also functions as part of the Walker Lane belt–eastern California shear zone, a dextral displacement system that accommodates 20–25% of the Pacific–North American relative plate motion (Unruh *et al.* 2003; Le *et al.* 2007). The Sierra Nevada microplate is moving coherently as part of the dextral displacement field of the eastern California shear zone.

The Sierra Nevada is most widely known for its prolific late Mesozoic magmatic arc history that generated the Sierra Nevada batholith (SNB). During the Cretaceous, the Great Valley constituted a forearc basin to the SNB. Magmatism of the SNB terminated in the medial Late Cretaceous. Arc magmatism spread across the northern to central Sierra Nevada region again in the Miocene (Busby *et al.* 2008a; Busby and Putirka 2009) placing the adjacent segment of the Great Valley again in an active forearc basin setting, although under primarily subaerial conditions as opposed to the marine conditions that dominated the late Mesozoic. Such Cenozoic arc magmatism is absent from the southern Sierra region, and, in parallel, mid-to-late Cenozoic depositional patterns of the southern Great Valley contrast with those of the central and northern Great Valley.

The San Joaquin Basin (SJB) is a distinct Neogene–Quaternary depocentre that developed along the southern ~150 km of the Great Valley (Addicott 1965, 1970; Bandy and Arnal 1969; Bartow 1984; Olson 1988; Bloch 1991a). In the late Oligocene through middle Miocene, the palaeo-shoreline environment extended along a WNW-ESE trace across the Great Valley from the palaeo-Sierra Nevada at ~36° N, and a shelf environment sloped SSW and dropped into a deep marine basin. To the north of the SJB, a thick mainly subaerial volcaniclastic wedge covered the western slopes of the Sierra and filled much of the Great Valley (Repenning 1960; Busby and Putrika 2009). The original eastern limits of the SJB are ill-defined adjacent to the current southern Sierra uplift, having been lost to uplift and erosion in the Quaternary. Its southern limits are known to have been in part controlled by growth faulting along the White Wolf fault (Goodman and Malin 1992), but are otherwise destroyed by the Pliocene–Quaternary rise of the San Emigdio–Tehachapi fold-thrust belt (Nilsen *et al.* 1973; Davis and Lagoe 1988). In the late Miocene, and again in the Pliocene, the geometry and resulting facies patterns of the SJB changed markedly in response to significant tectonic events including first the consolidation of the eastern escarpment fault system, and then the removal of mantle lithosphere from beneath the region (Saleeby and Foster 2004; Zandt *et al.* 2004; Le Pourhiet *et al.* 2006).

The Sierra Nevada microplate was defined on the assumption of its semi-rigid behaviour. This pattern breaks down south of 36.2° N, where it is extensively broken by the Neogene–Quaternary southern Sierra Nevada fault system. This system consists of intersecting normal and oblique slip transfer faults that strongly influence southern Sierra topography, and which also penetrate the eastern SJB forming the principal petroleum trap structures (Nugent 1942; San Joaquin Nuclear Project 1975; MacPherson 1978; Dunwoody 1986). Figure 2(a) shows the distribution of the principal members of the southern Sierra fault system. Figure 2(b) is a tectonic domain map for the same region as Figure 2(a), derived from the offset history of the fault system, as well as other tectonic features of the region, which are discussed below. Central to the focus of this paper is the northwestward widening basement uplift shown as the Breckenridge–Greenhorn horst. This actively growing structure is defined along its eastern margin by the Kern Canyon and related faults, and along its southwest margin by the Kern Gorge and related faults.

The Kern Canyon fault (KCF) constitutes one of the principal structures of the southern Sierra fault system. Having originated in the ductile regime in the Late Cretaceous (Busby-Spera and Saleeby 1990; Nadin and Saleeby 2008), the KCF has undergone brittle remobilizations in Neogene and Quaternary times. The Quaternary

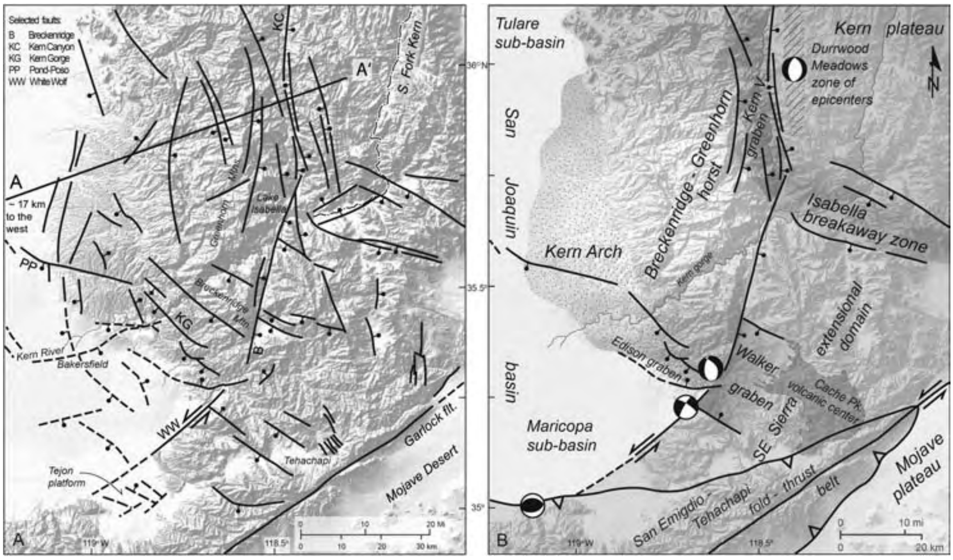

Figure 2. (a) Digital Elevation Model showing prominent normal, high-angle and oblique transfer faults of the southern Sierra Nevada fault system (after Smith 1964; Maheo *et al.* 2009, unpublished data). AA' is trace of Figure 3 cross-section. (b) Tectonic domain map for same region as Figure 2(a) showing domain-defining structures, epicentre zone of Durrwood Meadows seismic swarm and well-constrained earthquake focal mechanisms (Jones and Dollar 1986; Clinton *et al.* 2006; Lin *et al.* 2007), with dark quadrants representing compressional nodes.

phase of motion consists of west-side-up normal displacements along a series of scarps that produce a west tilt on the basement surface of the Breckenridge–Greenhorn horst (Nadin and Saleeby 2009; Maheo *et al.* 2009). This tilt pattern continues westwards in the subsurface of the adjacent SJB as a comparable west slope on the basement surface (Wentworth *et al.* 1995) as well as the regional west dip pattern of overlying Tertiary strata. In this paper, we review recent findings concerning the Quaternary history of the Kern Canyon and related faults, and the corresponding events in the adjacent SJB. These findings are integrated with regional relationships of the basement surface and Great Valley stratigraphy to the north, and together these relationships show that the principal controlling structure for the regional west tilt of the Sierra Nevada microplate steps over to the west at $\sim 36.4°$ N from the eastern escarpment system to the Kern Canyon system.

Overview of Sierra Nevada regional geomorphology

The geomorphology of the Sierra Nevada has been studied recently by field techniques, high-resolution digital elevation analysis, low-temperature thermochronometric techniques of apatite (U–Th)/He and fission track, and by cosmogenic dating of cave sediments and erosion surfaces (House *et al.* 1997, 1998, 2001; Reibe *et al.* 2000; Wakabayashi and Sawyer 2001; Stock *et al.* 2004, 2005; Clark *et al.* 2005; Cecil *et al.* 2006; Maheo *et al.* 2009). These studies recognize that following the Late Cretaceous termination of large-volume magmatism, the Sierra Nevada region underwent slow erosional denudation through the early Cenozoic to form a low-relief landscape with widely spaced, west-draining river canyons. The relict landscape surface is typically preserved along the broader interfluve surfaces of the main river drainages of the range as shown in Figure 1. The surface is characterized by low local relief, and is typically mantled by deeply weathered basement rocks with only local outcrops. Tors and short cliffs are common on hill slopes, especially at high elevations and in areas of widely spaced basement jointing. Small basins of coarse grus produced by hill slope weathering are common along stream segments that are separated by small basement exposures. In the southern Sierra, small isolated remnants of late Cenozoic volcanic rocks mantle the surface, which otherwise lacks cover strata (Smith 1964; Bergquist and Nitkiewicz 1982). In the central to northern Sierra, more extensive late Cenozoic volcanic sequences cover parts of the surface, and are also ponded into palaeo-canyons (Busby *et al.* 2008b; Busby and Putrika 2009). Along the west slope of the range, flat-topped interfluve surfaces are commonly weathered deeply to grus, representing erosional remnants of the surface, and in many locations such interfluve remnants map into the basal Eocene nonconformity of the Great Valley stratigraphic succession (cf. Unruh 1991; Wakabayashi and Sawyer 2001; Maheo *et al.* 2009).

During the Late Cretaceous–early Cenozoic, the Sierra Nevada region constituted the southwest margin of a regional orogenic plateau (Nevadaplano), from which the microplate was calved off during the westward migration of late Cenozoic Basin and Range extensional tectonism (Wernicke *et al.* 1988; Surpless *et al.* 2002; Busby and Putirka 2009). The relict landscape surface is interpreted as the erosionally modified western reaches of the plateau surface. Throughout the Sierra, this surface has undergone ~2–3 km of slow erosional denudation since the Late Cretaceous at a rate of ~0.04 mm per year in the northern to central Sierra (Clark *et al.* 2005; Cecil *et al.* 2006), and ~0.06 mm per year in the southern Sierra (Maheo *et al.* 2009). Early west-draining rivers that incised the surface were repeatedly filled by Tertiary volcanic–volcaniclastic strata, and then repeatedly re-incised (Busby *et al.* 2008b; Busby and Putirka 2009). An episode of accelerated basement incision along major west-draining river canyons began at post-20 Ma time (House *et al.* 2001; Clark *et al.* 2005; Clark and Farley 2007), presumably in response to microplate inception and regional west tilting. A second phase of accelerated river incision began at ca. 3.5 Ma, presumably in response to uplift driven by the foundering of the underlying mantle lithosphere (Saleeby and Foster 2004; Zandt *et al.* 2004; Le Pourhiet *et al.* 2006). These incision events, in concert with the eastern escarpment faulting, give the Sierra Nevada its overall morphologic character of mainly west-draining deep river gorges separated by broad low-relief interfluves. This pattern breaks down south of ~36.4° N, where the Kern River forms major south-draining branches that join in the Isabella Basin, where the main trunk bends southwestwards and continues across the KCF, incising sharply into basement and forming the lower Kern Gorge (Figure 2(a)).

The slow long-term erosion rates determined for the relict landscape surface by apatite He data are similar to short-term rates derived from cosmogenic dating of granitic surfaces on or near the surface (Reibe *et al.* 2000; Stock *et al.* 2005). Cosmogenic ages from cave sediments in the Kings River drainage (Stock *et al.* 2004) indicate a channel incision rate of 0.27 mm per year between 2.7 and 1.4 Ma, and volcanic capped river terraces in the central Kern River drainage suggest an average incision rate of 1.1 mm per year since 3.5 Ma (Dalrymple 1963; Ross 1986). These data directly record channel lowering, whereas the apatite He ages record an integrated erosion rate that encompasses both channel incision and local hill slope erosion. The high incision rate measured for the central Kern River drainage is intimately linked to the proximal effects of Quaternary normal faulting along the KCF, whereas the rate measured for the Kings River drainage reflects the propagation of the most recent erosional signal through the fluvial network arising from a regional relief increase.

Distinct changes in the morphology of the Sierra Nevada occur at ~38 and ~36.2° N, latitudes that bound the highest eastern crest of the range. Crest elevations decrease regularly northwards from ~38° N, and regularly but with a steeper gradient southwards from ~36.2° N. The San Joaquin and Kings Rivers constitute the deepest river canyons of the Sierra Nevada, with their headwaters reaching the highest eastern crest of the range (Figure 1). These canyons record substantial palaeo-relief (1000 m-scale) of probable Late Cretaceous age (House *et al.* 1998, 2001; Wakabayashi and Sawyer 2001). Palaeo-canyons further north in the Sierra exhibit palaeo-relief of 300–600 m (Busby *et al.* 2008b; Busby and Purtika 2009). Palaeo-canyons have not been resolved south of the Kings River drainage. From ~37° N northwards, the relict landscape surface lies in regional continuity with the basal Eocene nonconformity surface of the WSW-dipping Tertiary section of the eastern Great Valley (Unruh 1991; Wakabayashi and Sawyer 2001). The surface is ill-defined along the western margin of the range between ~37 and ~36° N, where, as discussed below, modern deformation is occurring. To the east, between 36.4 and 35.7° N, the surface takes a southerly tilt, south of where the surface is disrupted by extensive late Cenozoic faulting (Clark *et al.* 2005; Maheo *et al.* 2009). To the west, between 36.2 and 35.4° N, the surface assumes the west tilt of the Breckenridge–Greenhorn horst. Here, the surface also lies in continuity with the basal Eocene nonconformity of the eastern SJB (cf. Figure 3).

Geologic framework of the eastern SJB

The SJB is distinguished from much of the Great Valley by distinct facies relationships and palaeogeographic patterns that began at least as early as Oligocene time (Bandy and Arnal 1969; Addicott 1970; Bartow 1984; Bloch 1991a). Most notable, in distinction, is a SSW slope with a steeper gradient, as opposed to a WSW slope with a shallower gradient in the Great Valley to the north. Focusing on the eastern SJB: superimposed on the mainly Neogene SSW slope is the development of the Quaternary Kern arch, which has recently partitioned the eastern SJB into the Maricopa sub-basin to the south and the Tulare sub-basin to the north (Figure 2(b)).

The Kern arch is an actively growing topographic promontory that extends westwards into the SJB from the western Sierra, centred at latitude ~35.6° N (Figure 2(b)). It is extensively faulted, yet its underlying Tertiary section forms a west-dipping homocline (cf. Figure 3). It formed primarily in Quaternary time, with >1 km of Tertiary strata having been eroded from its eastern crest area, and progressively less erosion down to its transitions into the actively filling basin remnants (Dunwoody 1986; Maheo *et al.* 2009). The principal faults of the arch are east-side-up normal faults. Many smaller offset antithetic normal faults occur in association with the principal faults, some of which result in small grabens. Many more small offset faults cut the Kern arch than is shown in Figures 2(a) and 3. Total structural relief imposed across the crest of the arch by the basin dropping normal faults is ~4.5 to ~5 km over an ~40 km distance (Wentworth *et al.* 1995). This corresponds to an ~6–7° integrated west slope on the basement surface. Regardless of the intensely faulted state of the arch, its strata in general dip ~5–7° W with local variation of between ~20° W and ~3° E (California Department of Oil and Gas 1957; Dibblee *et al.* 1965; Dunwoody 1986; Figure 3).

The transition from the Kern arch into the Maricopa sub-basin consists of a series of NW-striking normal faults, the majority of which have had their SW walls down-dropped relative to the arch (Figure 2(a)). The Maricopa sub-basin contains up to ~10 km of post-85 Ma sediment in its deepest part, and drill holes as deep as 6.7 km only penetrate

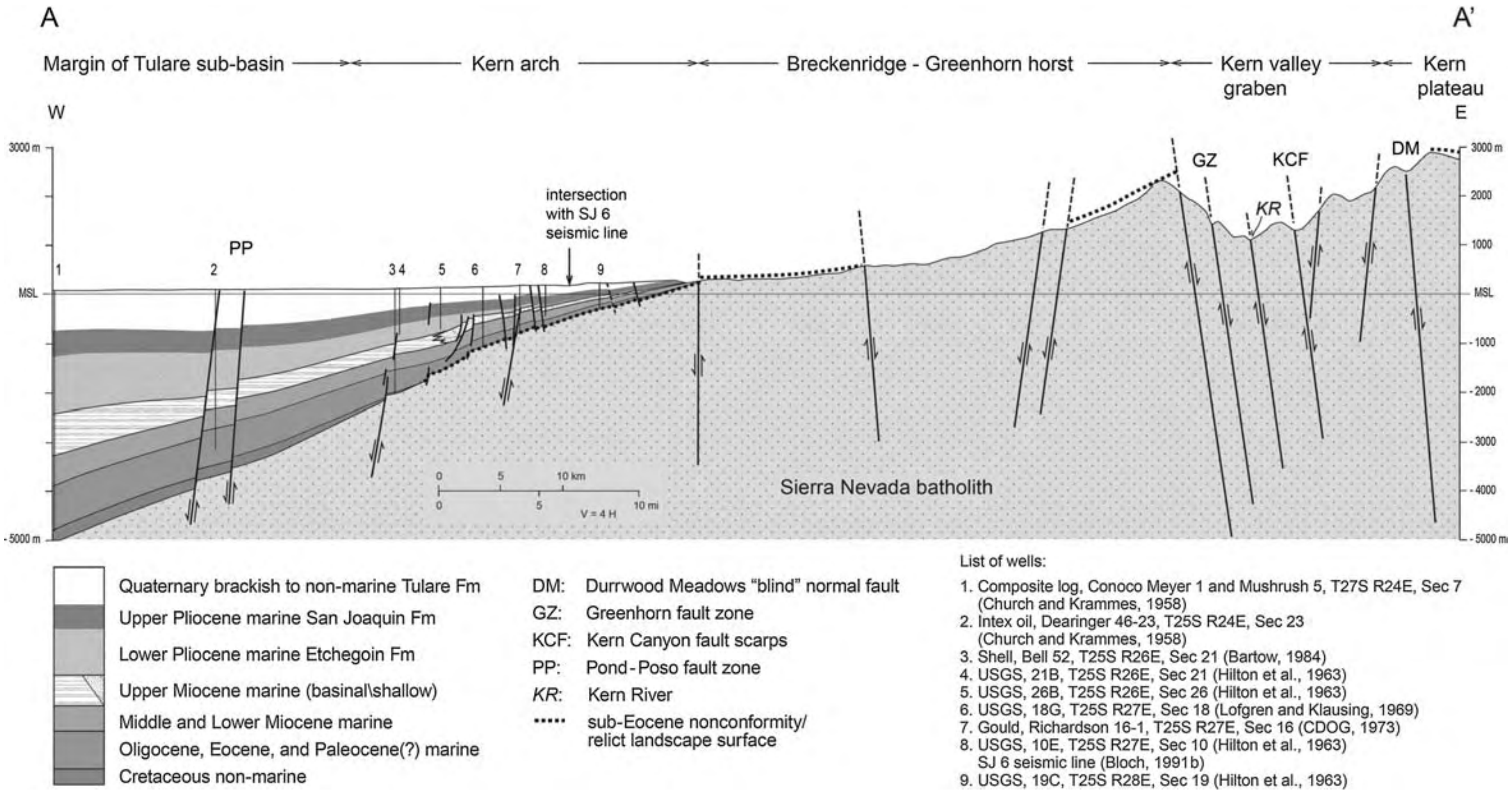

Figure 3. Cross-section between the southeast margin of the Tulare sub-basin and the west margin of the Kern plateau showing the generalized structure across the Kern arch and the Breckenridge–Greenhorn horst (section trace in Figure 1(a)). Topography along basement surface is averaged along 2-km-wide corridors that encompass the section line. Sources for subsurface data of the Kern arch and Tulare sub-basin are listed in the figure. The section was drawn oblique to the slope/dip of the horst/arch as per the availability of logged and cored wells.

to as deep as the middle Miocene (Goodman and Malin 1992). This sub-basin represents the deepest part of the eastern SJB. It is bounded to the south by the White Wolf fault, which along with the Kern Canyon system served as a Neogene oblique slip transfer zone separating differential extension in the sub-basin from that of the Tejon platform to the south and the SE Sierra extensional domain to the east (Figure 2). The Tejon platform is the remnants of a bank, relative to the sub-basin, that included Neogene strata of the western Tehachapi–San Emigdio Ranges, which in these ranges are undergoing uplift and erosion due to active fold-thrust tectonics (Nilsen *et al.* 1973; Hirst 1986; Goodman and Malin 1992).

To the north of the Kern arch sits the Tulare sub-basin. Unlike the Maricopa sub-basin, the Tulare sub-basin developed wholly in late Pliocene–Quaternary time partly coincident with the rise of the Kern arch (Davis and Green 1962; Miller 1999). Subsidence, at least in the eastern part of this sub-basin, is highly anomalous to all other areas of the Great Valley, with late Pliocene marine conditions spreading northeastwards across previous non-marine facies (Klausing and Lohman 1964; Lofgren and Klausing 1969), and Quaternary fluvial plain strata aggrading into the western Sierra Nevada and burying mountainous topography (Saleeby and Foster 2004). Within the western reaches of the Tulare sub-basin sits Tulare Lake, the last remnants of the once more extensive Corcoran Lake, which occupied much of the axial Great Valley in the Pleistocene. The residual Tulare Lake Basin and the embayment of the Tulare sub-basin into the regional elevated trends of the western Sierra Nevada are important epeirogenic features that will be discussed further below.

Evolution of the KCF system

The KCF system exhibits a polyphase movement history with evidence for distinct phases of motion in the Late Cretaceous, Miocene and Quaternary. It is the latest phase of motion that is the focus below, but earlier phases are important in terms of understanding the role of structural inheritance as well as the role of the system in influencing depositional patterns of the eastern SJB.

Cretaceous movement history

The Cretaceous movement history of the Kern Canyon system initiated between 100 and 96 Ma by reverse-dextral displacements along the southern SNB axis (Figure 1), while large-volume magmatism was still operative along the eastern margin of the SNB (Nadin and Saleeby 2008). This shear zone is defined as the proto-KCF (PKCF; Busby-Spera and Saleeby 1990). The PCKF and KCF coincide north of 35.7° N, but bifurcate to the south with the PKCF continuing southwards to the terminus of the range, and the KCF bending southwestwards and continuing into the White Wolf fault zone (Figure 1). Deformation along the PKCF was in the ductile regime producing a shear zone locally up to ~2 km wide. Tectonites recording this displacement regime can be traced as far north as ~36° N, north of where PKCF fabrics cannot be distinguished from the ductile fabrics of the KCF. Southwards the PKCF can be traced to the eastern Tehachapi Mountains, where steep east dips change progressively southwards to shallow east dips, and the shear zone merges at ~8 kb depths into shallow-dipping upper plate tectonites of the Rand subduction megathrust system (Wood and Saleeby 1998; Nadin and Saleeby 2008). The Rand subduction megathrust system lies as a broadly folded regional flat beneath the western Mojave Desert (Yan *et al.* 2005; Luffi *et al.* 2009). This megathrust descends northwards beneath the southern SNB as a regional-scale lateral ramp (Figure 1), projecting to Moho depths at ~35.5° N (Malin *et al.* 1994; Saleeby 2003).

At ca. 85 Ma, reverse-dextral shear along the southern segment of the PKCF ceased. Ductile to brittle dextral shear continued along the northern segment as far north as ~36.5° N. This dextral motion shunted out of the trace of the coincident PKCF–KCF south of 36.7° N, and continued southwestwards into ductile–brittle oblique dextral shear of the White Wolf zone. In this capacity, the Kern Canyon–White Wolf zone served as a transfer structure that partitioned the southernmost Sierra Nevada into two differentially SW–NE extending domains. To the southeast of the White Wolf zone, the western Tehachapi–San Emigdio batholithic rocks were exhumed up to ~10 kb (~35 km) depths (Pickett and Saleeby 1993; Saleeby *et al.* 2007; Chapman *et al.* 2008), whereas to the northwest batholith exhumation was up to ~4 kb (~14 km; Ague and Brimhall 1988; Nadin and Saleeby 2008). Thermochronometric data covering hot sub-solidus to low-temperature conditions indicate that the entire ductile history of the integrated P(KCF)–White Wolf zone was pre-80 Ma in age and at ca. 80 Ma exhumation rates south of 35.7° N changed dramatically from prior mm per year scales to 0.06 mm per year (Saleeby *et al.* 2007; Maheo *et al.* 2009, unpublished data); the later of which is comparable to Sierra-wide rates across the relict landscape surface to the north (House *et al.* 2001; Clark *et al.* 2005; Cecil *et al.* 2006).

Neogene movement history

Neogene–Quaternary brittle shear zones, faults and fault scarps are superimposed along the entire ductile damage zone of the KCF–White Wolf zone. The brittle shear fabrics are only loosely constrained to post-80 Ma in age, while structural, geomorphic and stratigraphic relationships record distinct phases of motion in the Neogene and again in the Quaternary. Somewhat cryptic is a distinct phase of early to middle Miocene growth and oblique transfer faulting recorded by sedimentation and volcanism along down-dropped walls of the integrated fault zone (Maheo *et al.* 2009). During this phase of motion, the Kern Canyon–Breckenridge segment of the zone bounded the western margin of an extensional domain in the southeastern Sierra Nevada, best defined by NW-striking normal faults of the Isabella breakaway zone and the Walker graben (Figure 2(b)). The 21–16 Ma Cache Peak volcanic centre (Evernden *et al.* 1964; Bartow and McDougall 1984; Coles *et al.* 1997) was nested in the eastern part of the Walker graben. Sediment-burial disturbance patterns of apatite He ages from the floor of the graben, in conjunction with constraints gained from down-hole temperature measurements in the SJB, indicate that ≥2.2 km of volcanogenic and siliciclastic sediments were ponded within the graben, with the Breckenridge segment of the fault system acting as a west bounding wall (Maheo *et al.* 2009). Sediments ponded in the Walker graben may have overfilled it and spread westwards into the eastern SJB as they overtopped the trace of the Breckenridge fault. More clearly is the channelling of Walker graben fill sediments through a structural depression broken across the Breckenridge–White Wolf zone, shown as the Edison graben in Figure 2(b). The Neogene course of what has been interpreted as the ancestral lower Kern River followed this depression into the SJB (MacPherson 1978).

A distinct phase of early to middle Miocene growth faulting, sedimentation and volcanism is also recorded in the subsurface of the Maricopa sub-basin and adjacent Tejon platform (MacPherson 1978; Hirst 1986; Goodman and Malin 1992). In this region, the White Wolf segment of the transfer zone partitioned differential extension along NW-striking normal faults of the sub-basin and platform. Vertical motion along the White Wolf zone resulted in the ponding of a thick Neogene section along its northern wall within the Maricopa sub-basin (Goodman and Malin 1992). Extension along the southern wall in the Tejon Platform continued northeastwards into that of the southeastern Sierra extensional domain (Figure 2(b)). Neogene graben fill thickness reconstructions for the Walker graben (Maheo *et al.* 2009) in conjunction with Neogene sediment thicknesses in the Maricopa sub-basin (MacPherson 1978; Goodman and Malin 1992) indicate that the Neogene Breckenridge–White Wolf transfer system had a scissors type of motion in its vertical offset components. The zero offset crossover in this scissors motion lies in the area of the Edison graben (Figure 2(b)).

Quaternary movement history

Prominent scarps bounding small alluviated basins run the entire ~130 km length of the KCF (Ross 1986; Nadin and Saleeby 2006, 2009; Nadin 2007). Geomorphic relationships, paucity of lateral stream offsets and seismic data indicate Quaternary, mainly west-side-up normal faulting. Late Quaternary scarps of the system have been mapped in detail between 35.5 and 36.2° N (Nadin 2007; Nadin and Saleeby 2009). Typically, there are multiple segmented scarps commonly connected by step-over scarps that suggest oblique transfer motion between adjacent segments. A survey of some of the scarps mapped is presented in Figure 4. Figure 4(a) is an aerial view northwards over Havilah Valley, centred at 35.5° N. In Havilah Valley, a well-developed, linear ridge of shattered basement ~1 km long and up to ~10 m high forms the western boundary of a flat alluvium-filled valley, indicating west-side-up displacement. Trenching through the hanging wall alluvium reveals an isotropic sediment mass with floating bed remnants suggesting deformation by liquefaction. The small scarp lies parallel to a more pronounced scarp to its west, which continues southwards out of the view of the photograph, into continuity with the principal Breckenridge scarp. Northwards, this escarpment forms the western prominent member of a set of three scarps that continue northwards over mountainous terrane to Isabella Basin (Figure 4(a)). The Engineer Point scarp that protrudes northwards into Lake Isabella is visible in the background. Figure 4(b) shows a view southwards with the Engineer Point scarp in the foreground, adjacent to the earthen Isabella Dam. In the area of the dam, ~30 m of Quaternary sediments are bounded to the west by the scarp (Page 2005), and to the west the lower Kern Gorge is incised deeply into footwall basement. Southwards, the scarp climbs over mountainous terrane towards Havilah Valley. The prominent summit area in the upper right of the photograph is Breckenridge Mountain, the footwall of the Breckenridge segment of the escarpment system.

Aerial photographs taken further north along the KCF show similar patterns of multiple scarps and juxtaposition of footwall basement against Quaternary deposits. Figure 4(c) is a view north at ~36° N. Here, a series of scarp segments merge in an echelon geometry. Continuing northwards to ~36.1° N, a steeply north inclined view shows two prominent scarps (Figure 4(d)). The eastern scarp juxtaposes shattered granitic basement against a dissected Quaternary debris flow, which is likewise sheared along the fault trace (Nadin 2007). The western scarp cuts obliquely across lithologic contacts in the Durrwood metamorphic pendant forming steep-sided gullies and ridgeline topographic steps.

From the area of Figure 4(d) northwards to ~36.4° N, the main KCF trace occurs as a sharp linear feature on aerial images and DEMs (Figure 5). At ~36.15° N, the escarpment is capped by a 3.5 Ma ~100 m thick basalt (Webb 1946; Dalrymple 1963; Du Bray and Dellinger 1981). This relationship is the most commonly cited evidence for lengthy quiescence of the KCF in that there is no evidence for dextral offset of the ‘capping’ basalt. Recent field investigations, however, reveal that above the trace of the KCF the surface of the basalt is shattered across an ~15 m high west-side-up escarpment, along which a fresh

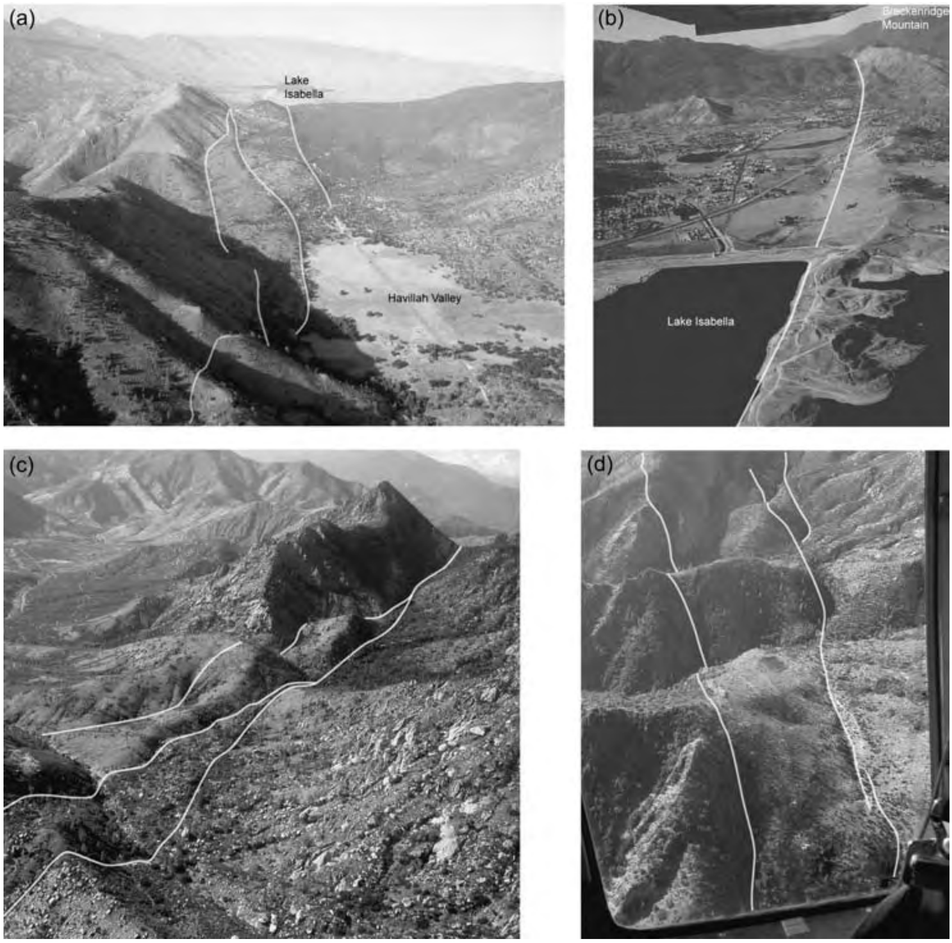

Figure 4. Oblique aerial photographs of various segments of the KCF zone displaying late Quaternary west-side-up normal scarp segments (photography by E.S. Nadin). (a) View north across Havilah Valley at $\sim 35.5°$ N; (b) view south from Isabella dam along Hot Springs Valley; (c) view north at $\sim 36°$ N and (d) near vertical north view at $\sim 36.2°$ N.

1–2 m scarp is locally preserved (Nadin 2007; Nadin and Saleeby 2009). Continuing northwards, at $\sim 36.2°$ N occurs Little Kern Lake, which was dammed by $\sim 0.2\,km^3$ of rock during earthquake-triggered slope failure (Townley and Allen 1939; Ross 1986). From the Little Kern Lake area northwards to $\sim 36.4°$ N, the KCF escarpment continues as a prominent geomorphic feature. Field investigations have not been performed recently along this northern segment of the escarpment, but they may resolve further evidence for late Quaternary normal displacements. North of $\sim 36.6°$ N, the geomorphic expression of the KCF diminishes abruptly.

Microseismicity is concentrated along the entire Breckenridge–KCF zone, as far north as 36.4° N (Southern California Seismic Network, catalogue data), with numerous larger ($M \sim 3$–4.9) events lying along the Durrwood Meadows seismicity patch, between 35.7 and 36.2° N (Jones and Dollar 1986; Clinton *et al.* 2006; Figure 2(b)). Such seismicity indicates that the Kern Canyon–Breckenridge zone is active, and that it is characterized by west-side-up normal displacements. A 2-week-long period of seismicity with >500

aftershocks occurred along the KCF in 1868, with the largest event assigned a value of $M = 6.5$ (Treasher 1949; Barosh 1969; Ross 1986). More recently (October 1983–May 1984), the Durrwood Meadows swarm consisted of >2000 events, many of which were $M \geq 3.0$, and the largest of which was $M = 4.9$ (Jones and Dollar 1986). The swarm was localized ~10 km east of the KCF (Figure 2(b)) and occupied an ~100 km long N–S vertical plane (Lin *et al.* 2007) with no evidence of ground breakage observed. All resolved focal mechanisms are consistent with pure west-side-up normal displacements at 0–7 km depths (Jones and Dollar 1986). All but one $M > 3.0$ event occurred between 4.0 and 5.9 km depths. On 14 April 2001, a well-constrained, shallow, $M = 4.1$ earthquake occurred ~10 km east of the KCF at latitude ~36° N. The focal mechanism indicates normal offset along a north-striking plane (Clinton *et al.* 2006) that coincides with the Durrwood Meadows patch (Figure 2(b)). The possible relationships between the Durrwood Meadows seismic swarm and the late Quaternary scarps that occur along the KCF are pursued further below.

Controlling structures for the rise of the Breckenridge–Greenhorn horst and the Kern arch

The Breckenridge–Greenhorn horst is defined as the northwest widening wedge-shaped basement uplift that produces the elevated areas of Breckenridge Mountain and the Greenhorn Mountains (Figure 2(a)). Structural relief of the horst is controlled by west-side-up normal displacements on the Kern Canyon and related faults and northeast-side-up displacements on NW-striking normal faults that terminate against the KCF system. The Kern arch constitutes the lower slopes of the horst, where Tertiary cover strata have yet to be eroded off to basement levels. Recent studies in apatite He thermochronometry, coupled to geomorphic and structural studies, have resolved offsets on the major structures that define the horst, and the related tilt patterns (Maheo *et al.* 2009). This study utilizes the geomorphic expression and thermochronometric tagging of the relict landscape surface (cf. Clark *et al.* 2005), as well as underlying palaeo-isothermal surfaces, to resolve structural relief and tilting related to high-angle normal faulting. Continuity between the relict landscape surface and the sub-Eocene nonconformity at the base of the eastern SJB Tertiary section facilitates direct correlation of structural relief patterns between the eastern SJB and the adjacent western Sierra basement.

Quaternary normal faults of the Kern Canyon system are segmented. The Breckenridge fault constitutes the southern segment of the system. Offset and tilt patterns of palaeo-isotherms as well as the relict landscape surface indicate a footwall west tilt of ~9° and an integrated west-side-up displacement of ~2.1 km. Stratigraphic relationships in proximal strata of the Kern arch, and apatite He age burial disturbance patterns suggest that a modest component of this 2.1 km of vertical displacement occurred during Neogene transfer faulting (Maheo *et al.* 2009). Quaternary normal faulting along the Breckenridge segment is concentrated along at least one and locally two principal scarps (Figure 2(a)). Northwards, this zone widens into a more diffuse zone of normal faulting, including the late Quaternary scarps of the KCF. Between ~35.7 and ~36.2° N, multiple west-side-up normal faults and subsidiary east-side-up normal faults produce the Kern Valley graben (Figure 2). Offset patterns and tilting of palaeo-isotherms and the relict landscape surface resolve an ~9° west tilt for the footwall domain west of the graben, and a minimum 600 m west-side-up displacement on the main segment of the Greenhorn fault zone that defines the west margin of the graben. The Greenhorn fault zone displays a 300–500 m escarpment along its trace, but with considerable erosional modification (cf. Figure 3).

Evidence of late Quaternary displacement has not been observed along the Greenhorn escarpment, although much of it is mantled with dense vegetation. Numerous topographic lineaments lie between and run parallel to the Greenhorn zone and the KCF scarps, and probably represent additional west-side-up normal faults. The late Quaternary scarps of the KCF lie mainly along the floor of the Kern Valley graben (Figures 2 and 3). The east wall of the graben is defined by an erosionally modified escarpment system, and offset palaeo-isotherms resulting from east-side-up normal faults with 400–500 m displacements (Figure 3). Further, east additional normal faults that parallel the graben cut the western edge of the Kern plateau. Some of these faults directly overlie the Durrwood Meadows seismicity patch (Figure 2). To the east, the Kern plateau is characterized by pervasive lineaments that parallel the KCF zone, but these have been poorly explored for Quaternary fault offsets.

The west tilt of the relict landscape surface across the Breckenridge–Greenhorn horst continues westwards as the faulted west-dipping homocline and basal nonconformity of the Kern arch Tertiary section. The Figure 3 cross-section is drawn at $\sim 35.9°$ N, where the west tilt pattern is controlled by diffuse normal faulting across the Kern Valley graben. Following the analysis of Jones and Dollar (1986), the Durrwood Meadows swarm is interpreted as an active west-side-up, blind normal fault. Numerous lineaments and normal faults lie above the Durrwood Meadows patch, but fresh west-side-up scarps have not been resolved, as they have for the KCF zone. The west to east sequence of the modified scarps of the Greenhorn zone, to fresh scarps of the KCF zone, to the seismically active blind faulting of the Durrwood Meadows zone suggests an eastwards migration pattern in the normal faults that control west tilting of the horst. This distributed zone of normal faulting in some manner circuits into the more spatially concentrated Breckenridge zone, possibly with transfer increments distributed along subsidiary NW- and NE-striking normal faults (Figure 2(a)).

Temporal constraints for the uplift and tilting of the Breckenridge–Greenhorn horst and the coupled Kern arch are provided by relationships in the eastern SJB. Upper Pliocene marine, and lower Quaternary fluvial and lacustrine strata are widespread and are intensely faulted across the northern arch, and extend northwestwards into the Tulare sub-basin (Klausing and Lohman 1964; Lofgren and Klausing 1969; Maheo *et al.* 2009; Figure 3). The tilting, emergence and erosional truncation of the upper Pliocene marine San Joaquin Formation provide the clearest lower age constraint on the Quaternary initiation for the growth of the coupled horst/arch. The additional presence of erosionally truncated lower Quaternary fluvial and lacustrine strata (Tulare Formation) could further indicate mainly late Quaternary initiation, although it could be argued that the lacustrine strata sampled by wells represent small lakes that formed in local grabens that were isolated from the extensive Quaternary lacustrine environment of the Tulare sub-basin.

The stratigraphic constraints on the growth of the coupled Breckenridge–Greenhorn horst and Kern arch posed above are consistent with the 3.5 Ma basalt ‘cap’ across the KCF along the upper Kern River being cut by a late Quaternary west-side-up scarp (Nadin 2007; Nadin and Saleeby 2009), as well as seismicity of the region (Jones and Dollar 1986; Clinton *et al.* 2006). Furthermore, permanent GPS stations of the southern Sierra Nevada region indicate that the horst is rising at mm per year scales relative to the Maricopa and Tulare sub-basins, as well as the hanging wall area of the horst within the Kern Valley graben (Nadin and Saleeby 2009). Such aseismic deformation could in Quaternary time alone generate the entire structural relief and tilt of the coupled horst/arch. Total relief across both the main Kern Valley as well as the upper stretch of the Kern Gorge is typically of the order of 1–1.5 km. With the average incision rate of 1.1 mm per year derived from the basalt 'cap' of the upper Kern, such relief could develop by erosion alone in ≤ 1.5 million years.

The southwest margin of the Breckenridge–Greenhorn horst is bounded by a set of NW-striking, northeast-side-up normal faults (Figure 2(a)). Such normal faults step down from the southwest margin of the horst into the Maricopa sub-basin. A diffuse zone of microseismicity extends along the trace of these horst-bounding structures, and intensifies near their intersection with the southern end of the Breckenridge fault (Southern California Seismic Network, catalogue data). Well-constrained focal mechanisms near the intersection zone indicate normal faulting along steep NW-striking surfaces (Clinton *et al.* 2006). Thus, the southwest bounding structures of the horst are likewise active. The Kern Gorge fault is a member of the NW-striking set, which has a well-developed late Quaternary northeast-side-up scarp (Gilbert 1928). Geomorphic, apatite He thermochronometric, and subsurface data indicate a northeast-side-up displacement of ~ 700 m on the Kern Gorge fault (Maheo *et al.* 2009). The Kern Gorge fault extends northwestwards into the SJB and merges with the Pond-Poso fault zone (Maheo *et al.* 2009). The southeast segment of this zone exhibits in the subsurface ~ 725 m northeast-side-up growth faulting over the past 1 million years, with evidence for modest Holocene displacement (Guacci and Purcell 1978). The Pond-Poso zone corresponds roughly to the inflection in the surface morphology of the Kern arch (Figure 2). This surface inflection resembles the hinge area of a broad open anticline, but all resolved structural relief arises from high-angle fault offsets, as opposed to bedding flexure. Topographic relief on the Kern arch as well as structural relief on the underlying basement surface (Wentworth *et al.* 1995) are the highest along the footwall area of the eastern Pond-Poso fault. Structure sections drawn across the Kern arch (Bartow 1984; Dunwoody 1986; Maheo *et al.* 2009; Figure 3) indicate that at least 1 km of Tertiary strata has been eroded off its crest area. Facies relationships and provenance data for the Tertiary strata, as well as broad structural constraints, indicate that the Tertiary section extended for a considerable distance across the exhumed basement of the horst prior to Quaternary uplift and erosion (Maheo *et al.* 2009; Figure 3).

Eastern Sierra escarpment to Kern Canyon step-over system

Regional tilt patterns

The west tilt of the Sierra Nevada has long been recognized as one of the principal morphotectonic features of California (Ransome 1898; Lingren 1911). Early recognition of this regional tilt pattern was based on the low west dips of Tertiary strata and volcanic rocks exposed along the western reaches of the relict landscape surface, and continuing westwards into the Great Valley. An essential element in this analysis is also the recognition of the westward thickening sedimentary prism that fills the Great Valley (cf. Hackel 1966), and subsequent subsurface mapping of the underlying west-dipping basement surface (Wentworth *et al.* 1995). The advent of apatite He thermochronometry coupled to geomorphic analysis has provided a structural datum on the Sierran basement surface that provides direct correlations to critical horizons within the Great Valley, thereby rendering a more complete picture of structural relief resulting from regional tilt. Structural relief of regional tilting is ultimately linked to west-side-up normal faulting along the eastern Sierra escarpment system, reaching from the Owens Valley margin in the south to the Honey Lake Valley margin in the north (Figure 1). Our recent findings show that this pattern breaks down south of $\sim 36.4°$ N, where the relict landscape surface acquires aberrant and variable slope patterns. Furthermore, fresh west-side-up-scarps

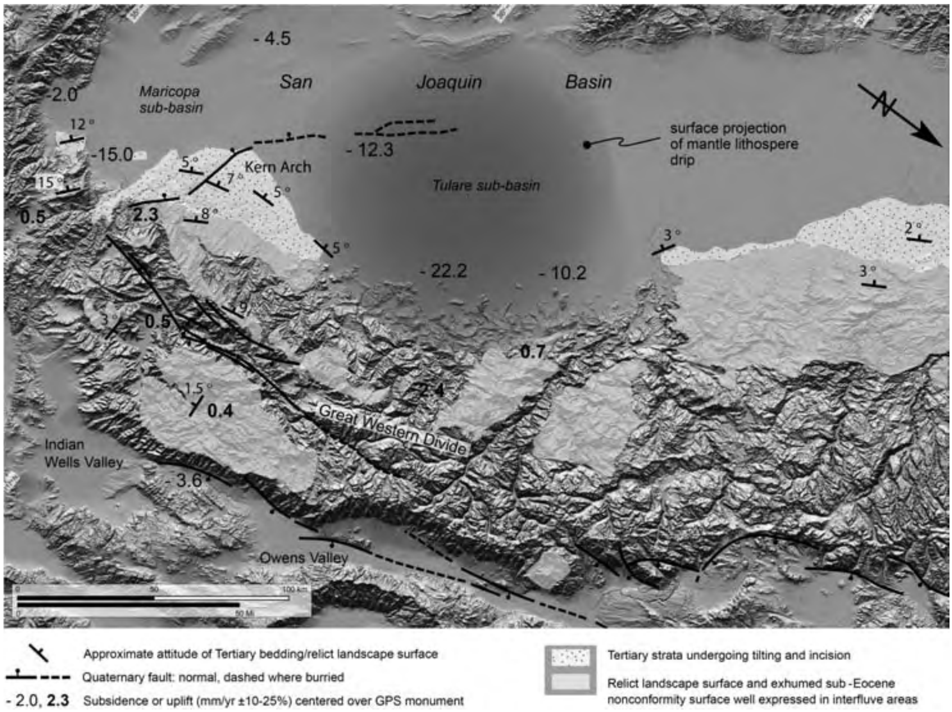

Figure 5. Digital Elevation Model of central to southern Sierra Nevada showing principal normal faults controlling regional west tilt pattern of microplate, generalized dips on relict landscape surface and Tertiary overlap strata, location of GPS stations for which vertical displacement rates have been published (Fay *et al.* 2008; Nadin and Saleeby 2009), and surface projection of mantle lithosphere drip (Jones *et al.* 1994; Ruppert *et al.* 1998; Zandt *et al.* 2004). Area for which relict landscape surface is well expressed after Clark *et al.* (2005) and Maheo *et al.* (2009). The image is oriented such that deformation along the eastern Tulare sub-basin is viewed down structure.

diminish along the western edge of southern Owens Valley, and are in general absent from the west margin of Indian Wells Valley (Figure 5). This further indicates a changing fault kinematic regime for the southern reaches of the microplate, at least in the Quaternary.

Geomorphic mapping and apatite He thermochronometry indicate that along the eastern Sierra, south of ~36.4° N, the relict landscape surface follows an integrated ~1.5° southerly slope, or tilt (Clark *et al.* 2005; Maheo *et al.* 2009), as opposed to the WSW regional slope/tilt that it follows to the north (Figure 5). This tilt pattern continues southwards through the Kern plateau to ~35.6° N, where the surface is disrupted by the Isabella breakaway zone, south of which only aberrantly oriented remnants remain scattered within the southeastern Sierra extensional domain (Figures 2 and 5). For the sake of brevity, the south tilted eastern Sierra domain is referred to below as the Kern plateau (Figure 2(b)). The Kern plateau and adjacent southeastern Sierra extensional domain are bounded to the west by the Quaternary KCF system, west of which sits the Breckenridge–Greenhorn horst. The west tilt of the horst is of the same sense as that of the greater Sierra Nevada to the north. Thus, at present, the controlling structure for the west tilt of the microplate south of ~36.4° N steps westwards from the eastern Sierra escarpment system to the Kern Canyon system. The amount and temporal relationships of tilting change across this transition in that the entire Tertiary section of the Kern arch typically dips ~ 5–7° (Figure 3), whereas to the north the dips of strata lying on the west flank of the range typically progress from ~ 1° for Pliocene up to ~ 5° for Eocene strata (Unruh 1991).

The regional west tilt pattern of the Sierra Nevada is distorted by late Quaternary deformation along the eastern margin of the Tulare sub-basin (Figure 5). The west tilt of the northern Kern arch is distorted northwards into the Tulare sub-basin. An analogous distortion pattern is observed along the northern margin of the sub-basin where the regional WSW dip of the Eocene Ione Formation, lying on the sub-Eocene surface, is deflected to a SSW dip, where it descends into the sub-basin (Figure 5). Figure 5 is laid out in such a fashion as to force the observer to view deformation along the eastern Tulare sub-basin down-plunge. The eastward embayment of the sub-basin into the western Sierra Nevada has resulted in the aggradation of fluvial plain sediments up into the valleys of the Kings, Kaweah and Tule Rivers, and the resulting burial of mountainous western Sierra topography. We emphasize that it is a fluvial plain, not alluvial fans, that are burying the mountainous topography. Thus, starting at ~ 37° N and extending southwards, the Sierra Nevada microplate is notably deformed internally, considering typical epeirogenic scales of deformation. Most notable are the embayment of Tulare sub-basin subsidence into the Sierran uplift, and the westward step-over in the controlling structure for regional west tilt from the eastern escarpment to the Kern Canyon system.

Timing of microplate inception and resulting topographic relief

In consideration of the timing of Sierra Nevada microplate inception, we focus first on the nature of the bounding structural systems. We recognize two fundamental types of boundaries in regard to their behaviour with respect to classical plate tectonic theory: well-defined classical plate boundaries and diffuse boundaries that defy, or complicate rigid plate kinematic analysis. The eastern Sierra escarpment system and the Garlock fault are treated as reasonable approximations to classic plate boundaries. The eastern escarpment system approximates in behaviour a rift edge to the Basin and Range province, and the Garlock fault approximates a transform boundary. By contrast, the Coast Range fold-thrust belt and San Andreas fault (San Andreas transpressive boundary) constitute a highly diffuse western boundary for the microplate. East-directed thrust faults that root beneath the Coast Ranges ramp up for at least 30 km towards the axis of the Great Valley (Wentworth *et al.* 1983; Namson and Davis 1988). Some of these thrusts are known to be active (1983 Coalinga Earthquake), and some are recognized to have initiated in Eocene time. Furthermore, the initiation of slip along the San Andreas fault is only broadly constrained to between middle Miocene and early Pliocene time (Dickinson 1996; Oskin and Stock 2003). Thus, temporal relationships along the San Andreas transpressive boundary are not likely to be very definitive for microplate inception. The northern boundary of the microplate is likewise a zone of active diffuse compressional deformation, reflecting NNW impingement of the microplate into the Klamath Mountains province across the Mendocino plate edge (Figure 1; Unruh *et al.* 2003; Hammond and Thatcher 2005). Thus, temporal relationships of the eastern Sierra escarpment system and the Garlock fault are the best structural indices available for microplate inception.

Late Miocene time and specifically ca. 10 Ma appear to represent the most definitive time for microplate inception. A combination of structural and stratigraphic relationships in Neogene volcanogenic strata capping the east-central to northern Sierra Nevada region indicate that extensional faulting migrated westwards to, and regionally coalesced into, the eastern escarpment system at ca. 10 Ma (Henry and Perkins 2001; Surpless *et al.* 2002; Busby *et al.* 2008b; Busby and Putirka 2009). Consistent with this timing is a vertical apatite He age transect through the footwall of the Mount Whitney region escarpment indicating rapid tectonic denudation at ca. 10 Ma (Maheo *et al.* 2004). Continuing southwards, the Indian Wells Valley segment of the eastern escarpment system provided an upland source for copious sediment shed eastwards into the El Paso Basin (Figure 1) by ca. 8 Ma (Loomis and Burbank 1988). This early phase of eastern escarpment faulting in the far south occurred in conjunction with the late Miocene initiation of sinistral motion along the Garlock fault (Loomis and Burbank 1988; Monastero *et al.* 1997). Eastern escarpment faulting in this region did not produce a resolvable west tilt to the relict landscape surface due to the fact that the surface was previously disrupted by Miocene extensional tectonism (Maheo *et al.* 2009), unlike regions to the north.

Data on the rejuvenation of river incision into Sierran basement as well as depositional patterns in the SJB are consistent with a ca. 10 Ma inception of the microplate. Apatite (U–Th)/He and ^{3}He/^{4}He data in conjunction with cosmogenic dating of cave sediments indicate initiation of the first major Cenozoic river incision event into basement in the southern Sierra between 20 and 3.5 Ma (Stock *et al.* 2004; Clark *et al.* 2005; Clark and Farley 2007). In apparent response to this event during the late Miocene, a series of regional plutono-clastic shallow marine sand sheets and derivative submarine fans began covering much of the SJB in conjunction with a marine regression along the eastern margin of the basin (Diepenbroch 1933; Bandy and Arnal 1969; Addicott 1970; MacPherson 1978; Bartow 1984; Hewlett and Jordan 1994). This flux of detritus included the delivery of sands into a marine embayment that extended from the SJB northwards along the axis of the mainly subaerial northern Great Valley (Repenning 1960). Production of copious plutono-clastic detritus is attributed here to the first phase of late Cenozoic river incision into basement, and the northern Great Valley marine incursion could signal the initiation of subsidence along the western reaches of the microplate in balance with the initiation of eastern escarpment faulting and regional west tilting. Incision into central to northern Sierra basement was to a great extent delayed until Pliocene time due to high base level in the northern to central Great Valley resulting from the production of volcaniclastic wedges which backfilled Sierran palaeo-canyons and covered the west slopes of the range (Busby and Piturka 2009).

Pliocene–Quaternary epeirogenic deformation

Geomorphic relationships and local structural relationships of volcanic flows lying along the west flank of the central to northern Sierra Nevada document the importance of Pliocene–Quaternary uplift and related WSW tilting of the microplate (Huber 1981; Unruh 1991; Wakabayashi and Sawyer 2001). Apatite He thermochronometry and cosmogenic dating reviewed above indicate that in the central to southern Sierra region this phase of uplift is the second in two stages of late Cenozoic uplift. Relationships between intra-canyon volcanic–volcaniclastic accumulations and inter-fill incision events permit an additional late Cenozoic uplift–incision phase in the central to northern Sierra region at ca. 15 Ma (Busby and Putirka 2009).

Turning to the Great Valley stratigraphic record, the ca. 10 Ma phase of uplift and incision is regionally expressed by the massive sand sheet of the SJB region and the coincident shallow marine incursion into the northern Great Valley, as outlined above. By contrast, no such sand sheet is expressed for the Pliocene phase, and aberrant activity for the Great Valley province is expressed only in the SJB area by a zone of anomalous subsidence along the eastern margin of the basin. This is readily observed in tectonic subsidence curves published for wells along the eastern margin of the Great Valley, where anomalous spikes are observed for wells only of the Tulare sub-basin area (Moxom and Graham 1987). Further south along the eastern SJB, direct evidence for anomalous Pliocene subsidence is obscured by the Quaternary rise and resulting erosion of the Kern arch. The anomalous morphology of the eastern Tulare sub-basin and the Kern arch relative to regional patterns of the western Sierra Nevada to the north are portrayed in Figure 6 as well as in Figure 5. In Figure 6, a regional tilt axis for the west-central Sierra Nevada is fit through the locus of points, where basement incision starts through the west-dipping Tertiary section along the major canyons of the Stanislaus, Tuolumne and Merced rivers. The bearing of this line matches regional strikes of the Tertiary section overlying the adjacent Sierran basement. The axis is extended southeastwards along the eastern margin of the Tulare sub-basin and up the northwest slope of the Breckenridge–Greenhorn horst, and is further used as the surface trace of the accompanying cross-section. The sediment surface along the eastern margin of the sub-basin consists of fluvial plain deposits. The generalized form of the buried mountainous topography beneath the aggraded fluvial sediments is generated by basement depths encountered for exploratory wells drilled along, or immediately adjacent to, the section trace (Wentworth *et al.* 1995). Distinct palaeo-topographic lows emerge on the cross-section, which could reflect the buried basement channels of the lower San Joaquin, Kings, Kaweah and Tule Rivers. The anomalous relief of the Breckenridge–Greenhorn horst, relative to the Sierran Foothills north of 37° N, is clearly expressed in the cross-section as well. This arises from the greater tilt of the horst, relative to the greater Sierra Nevada, and from the slight obliquity of the horst tilt axis relative to the tilt axis north of $\sim$37° N. Figures 5 and 6 together exhibit how strongly the southern Sierra Foothills region contrasts geomorphically with that of the central to northern Foothills region.

Late Pliocene–Quaternary subsidence in the Tulare sub-basin is linked in time to accelerated uplift and river incision in the adjacent Sierra Nevada, including the uplift and tilting of the Breckenridge–Greenhorn horst. Curiously, in contrast to the ca. 10 Ma acceleration in Sierran uplift and river incision, no massive regional sand sheet is recorded in the SJB for late Pliocene time. Instead muds, silts and fine sands of the shallow marine to paralic San Joaquin Formation record a marine transgression accompanied by an apparent starvation of locally derived coarse Sierran detritus. There are no constraints on how far east the San Joaquin Formation extended across western Sierra basement prior to the uplift of the Breckenridge–Greenhorn horst and adjoining western Sierra basement immediately east of the Tulare sub-basin. Geometric relationships displayed in Figure 3 and in cross-sections of Maheo *et al.* (2009) permit the possibility that late Pliocene shallow marine and paralic facies spread eastwards over much of, or the entire Breckenridge–Greenhorn horst. We will return to the distinctiveness of the upper Pliocene San Joaquin Formation and its depositional environment below.

The Tulare sub-basin sits above a vertical high-velocity slab that extends to $\sim$225 km depth into the upper mantle (Jones *et al.* 1994; Ruppert *et al.* 1998; Saleeby and Foster 2004). The slab is interpreted to be the foundered mantle lithosphere that prior to Pliocene time lay beneath the southern Sierra Nevada region (Figure 7). The slab is still attached to viscously deforming lower crust beneath the sub-basin (Zandt *et al.* 2004). The Pliocene–Quaternary phase of uplift in the southern Sierra Nevada region as well as roughly synchronous subsidence in the Tulare sub-basin are interpreted as dynamically coupled vertical displacements resulting from the mantle lithosphere foundering process. Thermo-mechanical models of such processes predict a complex pattern of vertical displacement transients with subsidence and uplift linked by migrating rolling hinges as lower crustal

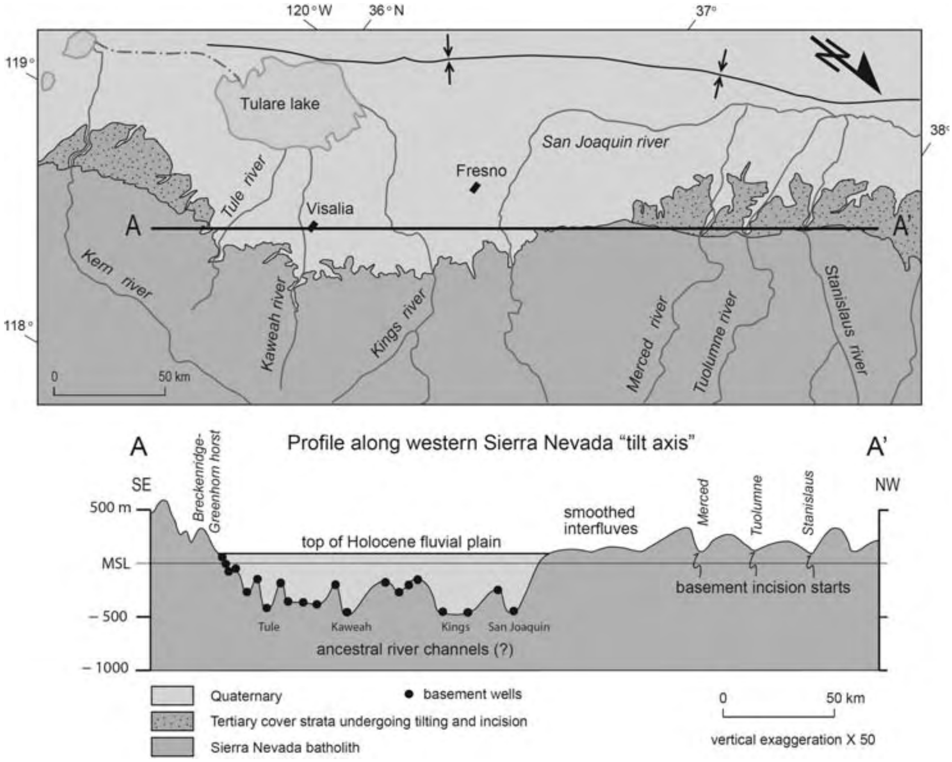

Figure 6. Cross-section drawn along trends of tilt axis of the western Sierra Nevada between ~37 and ~38° N, and extended southwards across the eastern edge of the Tulare sub-basin and northwest margin of the Breckenridge–Greenhorn horst. Basement depths in the Tulare sub-basin are after Wentworth *et al.* (1995).

viscous coupling and upper crustal flexure change as the mantle instability evolves (cf. Pysklywec and Cruden 2004; Le Pourhiet *et al.* 2006).

Tectonics of the eastern Sierra escarpment to Kern Canyon step-over and related landscape evolution

Mantle lithosphere foundering in the southern Sierra Nevada region

Multiple lines of evidence show that the southern SNB lost its underlying mantle lithosphere in the Pliocene. Most notable is a profound change in the Neogene–Quaternary volcanic hosted mantle xenoliths from mantle wedge assemblages of the SNB to shallow asthenospheric assemblages during a coincident change in the relatively low-volume late Cenozoic volcanic rocks erupted over the region to more primitive compositions (Ducea and Saleeby 1996, 1998; Farmer *et al.* 2002; Saleeby *et al.* 2003). The mantle wedge xenolith assemblage shows evidence of being conductively cooled, and forming the mantle lithosphere beneath the southern SNB over the latest Cretaceous and much of Cenozoic time. Seismic studies further show relatively thin crust lying above asthenospheric mantle in the region of the eastern Sierra–Owens Valley, Great Western Divide and Breckenridge–Greenhorn horst (Ruppert *et al.* 1998; Fliedner *et al.* 2000). The Moho *is* the lithosphere–asthenosphere boundary of these regions. By contrast, the area of the Tulare sub-basin and immediately adjacent western Sierra is underlain by thicker crust,

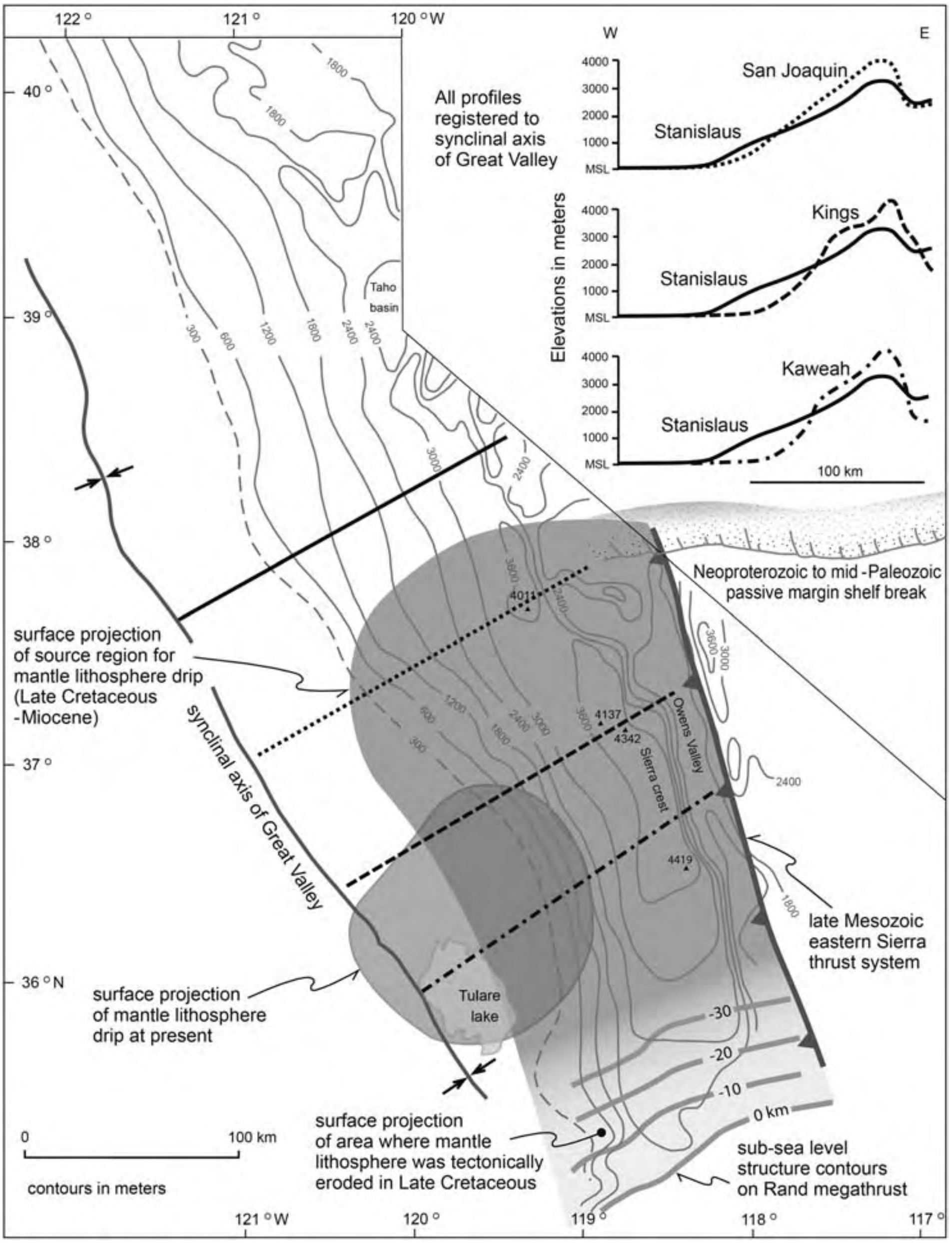

Figure 7. Contour map of regional averaged topography of the Sierra Nevada generated by contouring across major interfluves (modified after Wakabayashi and Sawyer (2001)). Also shown are regions underlain by high-density mantle lithosphere prior to its foundering, region currently underlain by foundered mantle lithosphere mass and other features referred to in the text. Inset shows averaged topographic profiles for select transverse corridors identified by adjacent river canyons.

and anomalously high-velocity lithospheric mantle that extends downwards to $\sim$225 km depths as a steep slab, or drip-like structure (Jones *et al.* 1994; Ruppert *et al.* 1998; Figure 5). Above this slab, much of the Moho is missing, or highly obscured, suggesting lower crust entrainment into the flow field of the actively foundering mantle lithosphere

(Zandt *et al.* 2004). One of the key findings of these studies is a concentration of high-density eclogitic batholithic residues/cumulates within the foundered mantle lithosphere, which in conjunction with thermal factors adds to its gravitational instability. Mantle xenolith data as well as trace element data on the SNB suggest that such eclogitic residues/cumulates were concentrated in the southern SNB, south of ~38° N (Dodge *et al.* 1982; Ross 1989; Ducea and Saleeby 1996, 1998; Ducea 2001). We suspect that this geographic variation reflects the palaeo-lithospheric structure of the SNB host in that the northern edge (shelf break) of the ~ E–W trending Neoproterozoic to mid-Palaeozoic passive margin extended into the palaeo-Sierra region at ~38° N (Figure 7) with its pre-batholithic transform truncation located along the western Sierra region (Davis *et al.* 1978; Kistler 1990; Saleeby 1992). Hence, the northern and southern segments of the SNB developed in contrasting source regimes with the thicker crustal regime in the south promoting a deeper integrated level of lower crustal melting that was primarily below the plagioclase and within the garnet stability fields.

Figure 7 shows the area over which mantle xenolith and SNB trace element data together indicate that volumetrically significant eclogitic residues/cumulates populated the mantle wedge at the time of the Late Cretaceous termination of large-volume SNB magmatism (Dodge *et al.* 1982; Ross 1989; Ducea and Saleeby 1996, 1998; Ducea 2001). The northern margin of this upper mantle domain is considered to have been transitional into mantle lithosphere that lacked such a high concentration of eclogitic residues, as discussed above. The western margin is defined by the western extent of basement wells that are dominated by SNB rock types (Saleeby 2007, unpublished data). The eastern margin is shown bounded by the late Mesozoic eastern Sierra thrust system (Dunne and Walker 2004), based on the analysis of Ducea (2001). The high-density mantle lithosphere was truncated to the south in the Late Cretaceous by tectonic erosion along the Rand megathrust, for which its northern ramp is shown as structure contours in Figure 7 (after Malin *et al.* 1995; Saleeby 2003; Yan *et al.* 2005). Thus, cool high-density mantle lithosphere lay beneath the southern SNB between ~35.5 and ~38° N from Late Cretaceous time until its foundering in the Pliocene. Figure 7 also shows the area that currently overlies the foundered mantle lithosphere, as imaged seismically (Jones *et al.* 1994; Ruppert *et al.* 1998; Zandt *et al.* 2004), and as shown in Figure 5.

A number of geomorphic and structural changes occur in the Sierra Nevada microplate across the boundaries between the upper mantle domains outlined above. This is observed in the smoothed topographic base of Figure 7, which was constructed by mechanical contouring across interfluve surfaces (modified after Wakabayashi and Sawyer 2001). Anomalously low elevations in the southern Sierra Nevada, and in parallel the anomalous deep palaeo-bathymetry in the SJB relative to the rest of the Great Valley, correspond to the region that lost its mantle lithosphere in the Late Cretaceous along the Rand megathrust. Furthermore, the southern Sierra Nevada fault system is concentrated in the same region, and dissipates northwards into regions that retained their mantle lithosphere until the Pliocene (Figure 2(a)). The region of the highest integrated elevations remained rooted into the high-density mantle lithosphere up to Pliocene time. This includes the axial to eastern Sierra south of 38° N as well as the area of the Breckenridge–Greenhorn horst and Kern arch. The Tulare sub-basin including its area of embayment into the western Sierra Foothills corresponds to the modern surface projection of the foundered mantle lithosphere. The more ideal regional morphology of tilted Sierran uplands transitioning westwards into the Great Valley sedimentary prism lies north of all of the above surface level and upper mantle complexities. We consider this northern Sierra domain to be the idealized form of the microplate with its generalized topographic profile derived from a corridor along the Stanislaus River area in Figure 7. This form is seen to transition southwards through the San Joaquin profile to more anomalous profiles of the Kings and Kaweah rivers that lie immediately adjacent to the foundered mantle lithosphere.

Diagrammatic and numerical models have been published depicting lithosphere foundering along transverse sections through the southern Sierra Nevada microplate and the adjacent area of the Basin and Range province (cf. Jones *et al.* 1994; Farmer *et al.* 2002; Saleeby *et al.* 2003; Zandt *et al.* 2004; Le Pourhiet *et al.* 2006). These models, to a first order, present a coherent picture of mantle lithosphere mobilization in the Pliocene with coincident changes in mantle composition, volcanism, eastern Sierra uplift and accelerated river incision into basement. These models further predict lingering anomalous subsidence in the Tulare sub-basin, whose underlying crust is still coupled to the foundered mantle lithosphere mass. Thermo-mechanical models that explore the mantle lithosphere foundering process in three dimensions are technically challenging, and only in early stages of development (Le Pourhiet *et al.* 2006, ongoing research).

Figure 8 presents a three-dimensional working model for the surface responses to southern Sierra Nevada region mantle lithosphere foundering. The pretence of this model

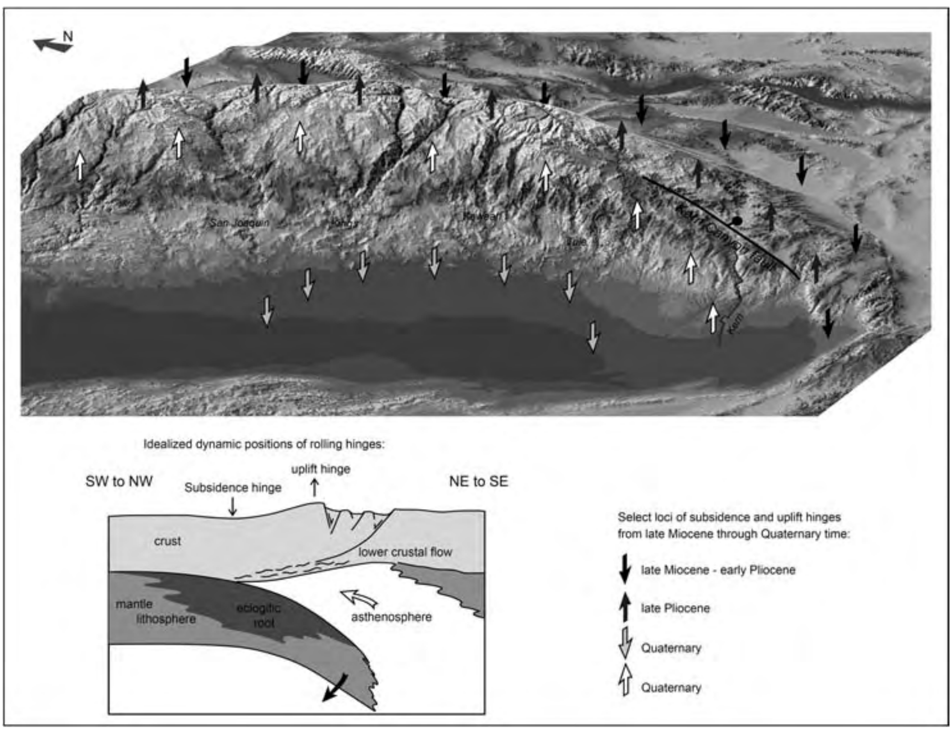

Figure 8. Oblique digital elevation model of the southern Sierra Nevada region showing generalized positions of subsidence and uplift rolling hinges for select times that migrated through the region in response to mantle lithosphere foundering based on thermo-mechanical modelling of Le Pourhiet *et al.* (2006), and constraints on Sierran landscape evolution and eastern San Joaquin subsidence and uplift patterns. Inset shows idealized positions of subsidence and uplift hinges in cross-sectional view in relation to progressive peeling away of mantle lithosphere and inflow of asthenosphere.

is that essentially the same processes operated in longitudinal or oblique sections as in the conventionally analysed transverse section. Vertical displacement transients induced by the progression of the foundering process are adopted from the two-dimensional models of Le Pourhiet *et al.* (2006). In these models, viscous drag on the lower crust induced by the peeling away of the mantle lithosphere first pulls a subsidence wave that migrates above the region of progressive mantle lithosphere detachment. As the mantle lithosphere progressively pulls away from the lower crust, the flexural response of the upper crust to being freed of viscous drag in conjunction with the inflow of buoyant asthenosphere induces uplift. Hence, in theory, at least two migrating rolling hinges passed through the region: first between the initial state and a subsidence wave, and then a subsequent uplift wave. The Figure 8 model uses the transverse temporal relationships outlined above, in conjunction with subsidence and uplift data along the southwestern Sierra–eastern SJB to hypothetically track in time and map view the migration of the initial subsidence wave and the subsequent uplift wave.

The subsidence–uplift analysis of Figure 8 successfully predicts a series of late Miocene–early Pliocene lake basins preserved along the Owens Valley, Indian Wells Valley and southernmost Sierra regions (Dibblee and Louke 1970; Bachman 1978; Bacon *et al.* 1982), as well as accelerated early Pliocene subsidence preserved off the south flank of the Kern arch, Maricopa sub-basin and Tejon platform (Dunwoody 1969; Goodman and Malin 1992). According to theory, the position of the late Miocene–early Pliocene subsidence hinge migrated to its Quaternary position, as shown in Figure 8, by passing through the intervening region. Any resulting sedimentary accumulations in these areas had little potential for preservation being within the area of subsequent uplift. In this context, we focus on some of the distinct features of the upper Pliocene San Joaquin Formation, where exposed along the north flank of the Kern arch. The muds, silts, and fine sands of these strata record a marine transgression that reached at least as far east as the western Sierra Foothills in the area of the Tulare sub-basin and northern Kern arch (Klausing and Lohman 1964; Maheo *et al.* 2009; Figure 3). The transgression was accompanied by an apparent starvation of locally derived coarse Sierran detritus. An important exception is granule size tonalitic to granodioritic detrital grus layers and diamictite disseminations that are present in the fine green mudstones and siltstones of the eastern exposures of the unit. We attribute the distinct nature and depositional setting of the eastern reaches of the San Joaquin Formation to the migration of the subsidence hinge into proximity of the eastern SJB margin, which decreased Sierran relief adjacent to the basin and ultimately pulled the strand line eastwards away from the principal depocentre of the basin. This pattern temporally starved the basin from coarse locally derived Sierran detritus. Shallow marine conditions are envisaged to have spread rapidly eastwards over the slowly denuding relict landscape surface thereby liberating and dispersing fractions of the widespread surface grus into the shallow marine fine sediments. Lacustrine and fluvial deposits of the Quaternary Tulare Formation overlie the San Joaquin Formation (cf. Figure 3), signalling the subsequent migration of the uplift hinge into the proximity of the Tulare sub-basin margin and the resultant marine regression.

The analysis of Figure 8 predicts that the uplift hinge, following in the wake of the subsidence hinge, migrated through the eastern Sierra region in the late Pliocene (ca. 3.5 Ma). Such migration continued to move the uplift hinge to beneath the Great Western Divide and Breckenridge–Greenhorn horst region by ca. 2 Ma elevating the Divide, horst and Kern arch. Concurrently, the subsidence hinge migrated into the Tulare sub-basin. Such vertical displacement transients are poorly resolved for the northern sector of the system, between 37 and 38° N. This could reflect a more dampened signal to the vertical transients as a result of a broader transition in the sub-SNB lithosphere structure that developed across the palaeo-lithosphere structure of the passive margin shelf break, as opposed to the regional thrust systems that had previously truncated the eclogitic root along the east and south edges of the southern SNB (Figure 7). A greater flexural strength along the central reaches of the microplate, relative to its structurally disrupted southern end and across transverse sections, could conceivably contribute to the dampening of the vertical transients along the northern sector as well.

Vertical motions for permanent GPS stations of the southern Sierra Nevada region (Fay *et al.* 2008; Nadin and Saleeby 2009) are shown in Figure 5. The highest measured positive verticals are in the Breckenridge–Greenhorn horst and Great Western Divide areas (2.3–2.4 mm per year). Large negative vertical motions are resolved for the Tulare and Maricopa sub-basins, although the magnitude of these negative values is suspect due to widely practised ground water removal procedures in the region (Lofgren and Klausing 1969). Nevertheless, the GPS data are consistent with the analysis offered in Figure 8, showing the highest positive values in areas where the modern uplift wave is centred, lower positives across the Kern plateau and Kern Valley graben, and a progression from high to lower positive, to negative vertical displacements progressing from the actively uplifting areas to the actively subsiding Tulare sub-basin.

Epeirogenic uplift and regional fault blocks

Theoretical treatments of the mantle lithosphere foundering process predict the type of epeirogenic transients depicted in Figure 8 (cf. Pysklywec and Cruden 2004; Le Pourhiet *et al.* 2006). Inversion of microseismicity into a regional strain field model for the southern Sierra region suggests flattening of the upper crust by horizontal extension (Unruh and Hauksson 2009). Such an active upper crustal strain pattern is consistent with the rise and flexure of the crust over asthenosphere that has filled into the void left by foundered mantle lithosphere, and in theory should entail normal faulting along a network of intersecting faults. The southern Sierra Nevada fault system exhibits such a geometry with its $\sim$ N–S, NW and NE fault sets and related fracture systems. Many more small faults, and dense fracture sets penetrate the area than is mapped in Figure 2(a). Furthermore, as displayed on DEMs (cf. Figure 2(a)), the Kern plateau is pervasively fractured with many fractures displaying micro-to meso-scale fault offsets. Such a dense distribution of high-angle faults and fractures over the region is likewise consistent with both the results of the microseismicity strain inversion, and the migration of epeirogenic vertical displacement transients through the region.

In such an upper crustal flattening by horizontal extension kinematic regime, the regionally continuous Owens Valley and the Kern Canyon normal fault systems appear to be at odds with the predicted distributed normal faulting pattern. We assert that structural inheritance has played a key roll in partitioning upper crustal extensional strain along these regional fault systems. Both the Owens Valley and Kern Canyon systems originated as regional Late Cretaceous dextral fault zones (Ross 1986; Kylander-Clark *et al.* 2005; Nadin and Saleeby 2008, 2009). Both of these regional Late Cretaceous structural systems constituted zones of major crustal weakness that readily remobilized as epeirogenic strain waves propagated through their traces and into their emerging footwall domains. Comparison of the smoothed topographic profiles of Figure 7 to the position of the modern uplift hinge in Figure 8 suggests that the epeirogenic swell that deforms the west slopes of the Kings and Kaweah profiles, which produces the Great Western Divide, also corresponds to footwall uplift along the Breckenridge–Greenhorn horst.

Late Cenozoic relief and Late Cretaceous Palaeo-relief

Contrasting views on the age of the principal topographic relief of the Sierra Nevada range from substantial old relief lingering from the Late Cretaceous (House *et al.* 1998, 2001; Poage and Chamberlain 2002) to primarily Pliocene–Quaternary uplift and relief production (Huber 1981; Wakabayashi and Sawyer 2001). The regionally averaged topography of Figure 7 shows that first-order Sierra Nevada topography is far from uniform. Elevations along the eastern Sierra crest and integrated across transverse sections are notably higher between ~36.4 and ~38° N than elsewhere. Palaeo-relief in this region is at its highest estimated value for the range, ≥1000 m (House *et al.* 2001; Wakaybayashi and Sawyer 2001), while dropping off north of ~38° N to 300–600 m (Busby and Putirka 2009). By contrast, Late Cretaceous palaeo-relief is not resolved south of ~36.4° N, where both the modern longitudinal topographic gradient and the depth of exhumation gradient are the greatest of the entire Sierra Nevada.

There is sufficient reason to suspect that, other than the relict landscape surface, there are no topographic features south of ~36° N that pre-date the Neogene. Our analysis suggests that the main branches of the Kern River are late Pliocene(?)–Quaternary features. The lower Kern Gorge is a superimposed valley with steep basement meander forms inherited from the river's course cut through the once overlying Tertiary section (Maheo *et al.* 2009). The upper main branch of the canyon is controlled primarily by Quaternary normal faulting along the Kern Canyon zone. Palaeo-relief along the base of the 3.5 Ma basalt 'cap' across the Late Cretaceous KCF zone reaches up to ~300 m over distances of ~3 km either side of the modern Kern channel, and is only feebly correlated to the modern drainage, if at all (Du Bray and Dellinger 1981). Furthermore, apatite He age transects across the upper Kern channel at ~36.4° N lack any signs of substantial palaeo-relief across the channel (House *et al.* 2001; Clark *et al.* 2005). Thus, the main channel of the upper Kern River and its lower trunk may be entirely controlled by Quaternary normal faulting along the KCF system. The west-flowing South Fork of the Kern River is controlled by Neogene normal faulting of the Isabella breakaway zone (Figure 2). Near the eastern end of the resulting Isabella Basin, the South Fork turns abruptly northwards and incises deeply into the relict landscape surface across the Kern plateau. It is possible that this south-flowing channel is an old feature following the southerly slope of the relict landscape surface off the flank of the palaeo-elevated region of Mount Whitney (i.e. House *et al.* 2001). This palaeo-Kern channel may have graded to sea level southwards, where a latest Cretaceous–early Palaeogene marine embayment spread eastwards across Late Cretaceous extensional terrane that developed above the Rand megathrust in the western Mojave region (Cox 1987; Lucas and Reynolds 1991; Wood and Saleeby 1998; Monastero *et al.* 2002; Saleeby 2003; T.H. Nilsen, personal communication 2004). We assume that the southerly slope of the relict landscape surface across the Kern plateau once extended to the marine embayment strand line, prior to its Neogene disruption. The Neogene river channel that entered the SJB through the Edison graben, which has been interpreted as the ancestral lower Kern (MacPherson 1978), was sourced within the Walker graben region (Figure 2(b)). This is shown by provenance data of the derivative conglomerate clast populations and detrital zircon U/Pb ages in fluvial strata in the eastern SJB (Z. Saleeby, unpublished data 2009).

Estimates of Late Cretaceous eastern Sierra crest elevations for the headwater region of the ancient Kern and Kings Rivers were calculated at ~1500 ± 600 m based on the assumption that these rivers, in their current channels, graded to sea level near the western margin of the range (Clark *et al.* 2005). Subsequent work shows that this analysis needs modification. First, we now reject the notion that the modern Kern River channel existed in the Late Cretaceous, which negates the internal consistency argument between results calculated for both the Kern and Kings headwater regions. Second, our recent survey of the SJB subsurface indicates that the Mid-to-Late Cretaceous shoreline environment lay typically $\sim$50 km to the west of the current range front in the southern Sierra Nevada region (cf. Figure 3; Ingersoll 1978; Reid 1988; Saleeby 2007). An $\sim$50 km westward translation of the reconstructed palaeo-Kings profile of Clark *et al.* (2005, Figure 5) is more consistent with crest regional elevations of $\geq$2000 m in the Late Cretaceous. Based on long wavelength palaeo-relief resolved in apatite He data from the San Joaquin and Kings river drainages, and comparisons with modern orogenic plateaus, House *et al.* (2001) suggested the headwaters of these palaeo-drainages issued from Nevadaplano elevations of $\sim$3000 m. Thus, in the following analysis, we use a value of $\sim$2500 $\pm$ 500 m for Late Cretaceous palaeo-elevation along the region of the palaeo-eastern Sierra crest, south of $\sim$38° N.

We now pursue a first-order analysis of the regional topographic variations along the Sierra crest region with time. We do so by deconvolving three principal components to relief generation: (1) epeirogenic uplift resulting from mantle lithosphere foundering; (2) tilting of the microplate resulting from regional plate tectonic processes; and (3) palaeo-relief lingering from the Late Cretaceous. Thermo-mechanical modelling of the lithosphere foundering process for the southern Sierra region suggests that $\sim$600 m of elevation increase occurred along the Sierra crest region due to mantle buoyancy redistributions as asthenosphere replaced foundered mantle lithosphere (Le Pourhiet *et al.* 2006). We assume that this elevation increase affected primarily the region that lost its high-density mantle lithosphere root, roughly 35.5° N to 38° N. Thus, in Figure 7, one could visualize the 3000 m contour as approximating the eastern crest regional elevation arising from the sum of microplate processes and palaeo-relief, with the Mt Whitney area possibly culminating as high as $\sim$3800 m.

The partial decoupling of the epeirogenic and microplate elevation increase signals is not unfounded. An important finding of the modelling of Le Pourhiet *et al.* (2006) is the metastable state that the high-density mantle lithosphere existed in throughout much of the Cenozoic, as a result its low thermal gradient inherited from Late Cretaceous time (Ducea and Saleeby 1996, 1998; Saleeby *et al.* 2003). A necessary condition for the mobilization of this cool rigid upper mantle layer was the migration of the Mendocino triple junction and the opening of a slab window beneath the region. The Mendocino plate edge migrated northwards through the Sierra Nevada region between ca. 25 and 4 Ma, and in its wake young oceanic microplates and slab windows were subducted and opened beneath the region (Atwater and Stock 1998). This migration pattern also entailed a relative plate motion change from transtensional to nearly pure transform at ca. 8 Ma. We infer that it was a combination of these plate tectonic processes that instigated Sierra Nevada microplate formation, and that its regional elevation increase and west tilt reflect its regional gravitational equilibration with the rapidly evolving upper mantle of the region. We further infer that such tilt and uplift were to a first-order uniform along the length of the microplate. This would imply that tilt-related elevation increase is of the order of $\sim$1000 m along the eastern Sierra crest.

Theoretical considerations and an array of geological observations indicate that additional epeirogenic transients affected the Sierra Nevada microplate during the early Neogene. The modelling of Le Pourhiet *et al.* (2006) suggests second-order vertical displacement transients during the early stages of mantle lithosphere mobilization in the early to middle Miocene, and theoretical treatments of triple junction migration suggest the related migration of vertical displacement transients through the region (Furlong and Schwartz 2004). Such early to middle Miocene transients are expressed by a shoaling to deepening cycle and associated volcanism in the eastern SJB (Bandy and Arnol 1969; Hirst 1986; Olson 1988; Bloch 1991a; Goodman and Malin 1992), distributed normal faulting and volcanic graben formation in the southern Sierra (Maheo *et al.* 2009), and re-incision of palaeo-channels in the central Sierra region (Busby *et al.* 2008b; Busby and Putrika 2009). These are considered important local epeirogenic transients, but perhaps of second-order importance in terms of late Cenozoic regional elevation increase as compared with uplift arising from the ca. 10 Ma microplate inception and tilting, and the ensuing mantle lithosphere foundering.

Figure 9 restores the Sierra Nevada microplate into its Late Cretaceous position as the western margin of the Nevadaplano (after Wernicke *et al.* 1996; Wernicke and Snow 1998). The palaeo-Sierra Nevada is rendered as smoothed topographic contours derived from Figure 7 by the subtraction of elevation increase increments resulting from microplate tilt and mantle lithosphere foundering registered to palaeo-relief estimates of the southern Sierra crest (House *et al.* (2001); and modifications after Clark *et al.* 2005). Late Pliocene–Quaternary subsidence along the eastern SJB and the rise of the Breckenridge–Greenhorn horst are also restored by retro-deforming the basement surface shown in Figure 6 to a linear trace, and by mating the relict landscape surface of the horst with that of the Kern plateau across the Kern Valley graben. The Mt Whitney area is shown culminating at $\sim$3000 m with the trace of the future eastern crest to the north descending northwards and ultimately grading to the Hornbrook marine basin that embayed into the northward projection of the palaeo-Sierran trend (Nilsen 1993). Upper Cretaceous shallow marine strata transitional between the northern Great Valley Group and strata of the Hornbrook Basin lie nonconformably on the northwestern Sierra basement pinning the Late Cretaceous shoreline environment to that area. The southerly trace of the shoreline environment followed a diagonal course across the Great Valley (Ingersoll 1978; Reid 1988).

The steeper south-directed topographic gradient off the Mt Whitney region is shown passing into the marine embayment that developed in the western Mojave region due to regional extension above the Rand megathrust (Wood and Saleeby 1998; Saleeby 2003). The southeast swing of the topographic contours to the south of the palaeo-Death Valley region reflect the continuation of the Nevadaplano through the palaeo-elevated area of the current Colorado plateau (cf. Huntington *et al.* 2009). The transition between the Mojave marine embayment and the southern Great Valley forearc basin consisted of a borderland environment that developed above westwards-displaced extensional allochthons of the SNB and its continuation into the northern Mojave (Wood and Saleeby 1998; Saleeby 2003). Much of this borderland record is preserved in the latest Cretaceous–early Palaeogene coarse marine strata of Salinia, displaced northwards from the southernmost Sierra Nevada–western Mojave region (Figure 1; Grove 1993; Schott and Johnson 2001). The Late Cretaceous–early Palaeogene regional extensional environment of the southernmost Sierra–northern Mojave region is extended northwards along the western Great Valley forearc–Franciscan transition to the area of the Stockton fault (Imperato 1995; Schemmann *et al.* 2007; Unruh *et al.* 2007). An important result of this regional supra-subduction extensional regime was the initial assent and exhumation of the previously underplated subduction assemblages of the entire western Mojave–Salinia, southern Sierra and southern Coast Ranges region (Jayko *et al.* 1987; Saleeby 2003; Saleeby *et al.* 2007; Schemmann *et al.* 2007; Unruh *et al.* 2007).

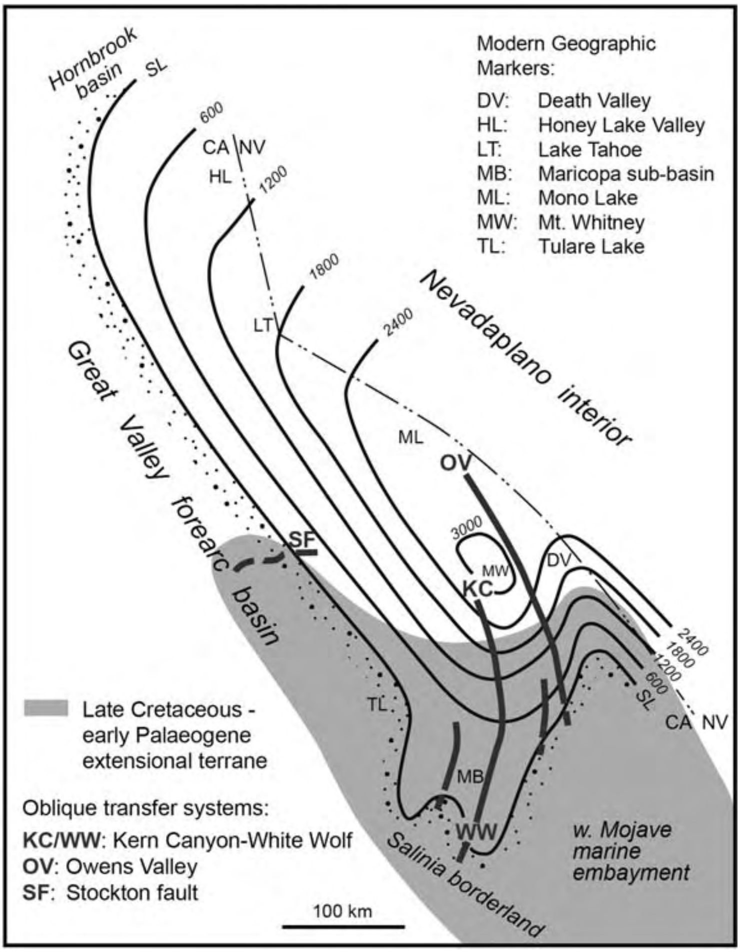

Figure 9. Diagrammatic smoothed topographic contour map constructed by subtracting out idealized elevation increase of the Sierra Nevada arising from microplate regional tilting and more localized mantle lithosphere foundering south of $\sim 38^\circ$ N (see text). The microplate is further restored into its Late Cretaceous position as western margin of Nevadaplano showing northern and southern marine embayments, southern Sierra–Mojave–Salinia extensional terrane and Kern Canyon/Owens Valley transfer fault systems. Sources referenced in the text.

The KCF–White Wolf zone and the proto-Owens Valley fault zone are also shown in Figure 9. The KCF–White Wolf zone was an important transfer structure during large magnitude Late Cretaceous extension, with extension nucleating above the Rand megathrust ramp in the southern Sierra and dispersing upper crustal extensional allochthons southwestwards above the region of the megathrust flat of western Mojave–Salinia. Recent work along the Owens Valley fault system indicates that it also functioned as a dextral fault during the Late Cretaceous, and that it very likely partitioned Late Cretaceous differential extension of the southern Sierra region from that of the southern Death Valley region (Applegate and Hodges 1995; Wood and Saleeby 1998; Bartley *et al.* 2003; Kylander-Clark *et al.* 2005). This relationship indicates that the step-over relationship between the Owens Valley fault system and the Kern Canyon system was established in the Late Cretaceous, which preconditioned the crust for the Quaternary step-over relationship.

Conclusions

Regional west-side-up normal fault control for the west tilt pattern of the Sierra Nevada microplate steps westwards at ~36.4° N from the eastern Sierra escarpment system to the Kern Canyon system. These regional tilt patterns are expressed by the slope of a regional relict landscape surface that developed by the slow erosional denudation of the western margin of the Nevadaplano, the southern segment of a Cordilleran wide orogenic plateau that developed in the Late Cretaceous–early Tertiary, and from which the Sierra Nevada microplate calved off in the Neogene. The regional west tilt patterns are further expressed by homoclinal Tertiary strata that lie nonconformably on the westward extension of relict surface as the latter descends off the west flank of the Sierra Nevada and continues beneath the sedimentary prism that fills the Great Valley. East of the Kern Canyon system, the relict landscape surface slopes southward, which at regional scales is an aberrant attitude that reflects the development of a marine embayment above a Late Cretaceous extensional terrane that cut into the western margin of the Nevadaplano in the southernmost Sierra–Mojave region.

The Sierra Nevada microplate is behaving as a semi-rigid lithospheric plate along its northern ~450–500 km stretch, but has been – and is – deforming internally along its southern ~100–150 km stretch. Non-rigid behaviour in the south arises from the crust having undergone profound deformation in the Late Cretaceous above a lateral ramp in the Rand subduction megathrust system. Above this megathrust ramp, the southernmost Sierra lost its mantle lithosphere, was internally imbricated along the proto-KCF, was progressively exhumed southwards to greater crustal depths and in series was pervasively broken by extensional structures. The KCF and its southwest extension as the White Wolf fault formed over the ductile-to-brittle regime as an oblique transfer system during the Late Cretaceous extensional regime. This transfer system was remobilized in the early Neogene during which it partitioned differential extension between the SJB and the southeastern Sierra Nevada.

The Kern Canyon zone was again remobilized in the Quaternary as series of west-side-up normal fault segments. Normal displacement along this zone has imparted an ~9° west tilt on the relict landscape surface that continues westwards into the eastern SJB as the west-dipping basal Eocene nonconformity surface, and is further expressed in comparable west dips of the overlying Tertiary section. The tilted basement surface is defined as the Breckenridge–Greenhorn horst, with its lower slopes still mantled by actively eroding Tertiary strata of the Kern arch. The Kern arch passes northwards into the Tulare sub-basin, a zone of anomalous Late Pliocene–Quaternary subsidence relative to all other segments of the eastern to axial Great Valley. Quaternary remobilization of the pre-weakened KCF zone, rise of the Breckenridge–Greenhorn horst and Kern arch, and anomalous subsidence in the Tulare sub-basin resulted from the Pliocene–Quaternary foundering of the southern Sierra mantle lithosphere that was left truncated along the Rand megathrust system, and which existed in a gravitationally metastable state from the latest Cretaceous through Miocene time beneath the southern Sierra region.

Acknowledgements

Discussions with Marin Clark, Tor Nilsen, Laetitia Le Pourhiet, Jeff Unruh, and John Wakabayashi were helpful for this synthesis. Critical reviews by Cathy Busby and Brian Wernicke are kindly acknowledged. Our research compiled in this synthesis was made possible by NSF grants EAR 0230383 and 0606903, and funds from the Gordon and Betty Moore Foundation. Caltech Tectonics Observatory Contribution no. 105.

References

Addicott, W.O., 1965, Miocene macrofossils of the southeastern San Joaquin Valley, California: United States Geological Survey Professional Paper 525-C, 101–109.

Addicott, W.O., 1970, Miocene Gastropods and biostratigraphy of the Kern River area, California: United States Geological Survey Professional Paper 642, 174 p, 21 pl.

Ague, J., and Brimhall, G.H., 1988, Magmatic arc asymmetry and distribution of anomalous plutonic belts in the batholiths of California – Effects of assimilation, crustal thickness, and depth of crystallization: Geological Society of America Bulletin, v. 100, p. 912–927.

Applegate, J.D.R., and Hodges, K.V., 1995, Mesozoic and Cenozoic extension recorded by metamorphic rocks in the Funeral Mountains, California: Geological Society of America Bulletin, v. 107, p. 1063–1076.

Argus, D.F., and Gordon, R.G., 1991, Current Sierra Nevada–North America motion from very long baseline interferometry: Implications for the kinematics of the Western United States: Geology, v. 19, p. 1085–1088.

Atwater, T., and Stock, J., 1998, Pacific – North American plate tectonics of the Neogene southwestern United States: An update, International Geological Review, v. 40, p. 375–402.

Bachman, S.B., 1978, Pliocene–Pleistocene break-up of the Sierra Nevada–White-Inyo Mountains block and formation of Owens Valley: Geology, v. 6, p. 461–463.

Bacon, C.R., Giovannetti, D.M., Duffield, W.A., Dalrymple, G.B., and Drake, R.T., 1982, Age of the Coso Formation, Inyo County, California: United States Geological Survey Bulletin 1527, 37 p.

Bandy, O.L., and Arnal, R.E., 1969, Middle Tertiary basin development, San Joaquin Valley, California: Geological Society of America Bulletin, v. 80, p. 783–820.

Barosh, P.J., 1969, Use of seismic intensity data to predict the effects of earthquakes and underground nuclear explosions in various geologic settings: United States Geological Survey Bulletin, Report, B1279, 93 pp.

Bartley, J.M., Friedrich, A.M., Glazner, A.F., Coleman, D.S., and Kylander-Clark, A., 2003, Large Laramide dextral shear across Owens Valley, eastern California, and extensional unroofing of the southern Sierra Nevada: Geological Society of America Abstracts with Programs, v. 35, no. 6, p. 305.

Bartow, J.A., 1984, Geologic map and cross sections of the southeastern margin of the San Joaquin Valley, California: United States Geological Survey Miscellaneous Investigations Series Map I-1496, scale 1:125,000.

Bartow, J.A., and McDougall, K., 1984, Tertiary stratigraphy of the southeastern San Joaquin Valley, California: United States Geological Survey Bulletin, v. 18, 1529 J, 41 p.

Bergquist, J.R., and Nitkiewicz, A.M., 1982, Geologic map of the Domeland Wilderness and contiguous roadless areas, Kern and Tulare counties, California: United States Geological Survey Miscellaneous Field Studies Map MF-1395-A, scale 1:48,000.

Bloch, R., 1991a, Studies of the stratigraphy and structure of the San Joaquin basin [Ph.D. Dissertation]: California, Stanford University, 319 p.

Bloch, R., 1991b, West coast regional cross section, San Andreas fault to Sierra Nevada Range: American Association of Petroleum Geologists, sheet 3.

Busby, C.J., and Putirka, K., 2009, Miocene evolution of the western edge of the Nevadaplano in the central and northern Sierra Nevada: palaeocanyons, magmatism and structure: International Geology Review, v. 51, p. 670–700.

Busby-Spera, C., and Saleeby, J.B., 1990, Intra-arc strike-slip fault exposed at batholithic levels in southern Sierra Nevada, California: Geology, v. 18, p. 255–259.

Busby, C.J., Hagan, J.C., Putirka, K., Pluhar, C.J., Gans, P.B., Wagner, D.L., Rood, D., DeOreo, S.B., and Skilling, L., 2008a, The ancestral Cascades arc: Cenozoic evolution of the central Sierra Nevada (California) and the birth of a new plate boundary: Geological Society of America Bulletin, v. 120, p. 331–378.

Busby, C.J., DeOreo, S.B., Skilling, I., Gans, P.B., and Hagan, J.C., 2008b, Carson Pass-Kirkwood paleocanyon system: Paleogeography of the ancestral Cascade arc and implications for landscape evolution of the Sierra Nevada, California: *in* Wright, J.E., and Shervais, J.W., eds., Ophiolites, arcs and batholiths: A tribute to Cliff Hopson. Geological Society of America Special Paper 438. v. 120, p. 274–299.

California Department of Oil and Gas, 1957, Summary of Operations, California Oil Fields: Mount Poso Field, v. 43 no. 2.

Cecil, M.R., Ducea, M.N., Reiners, P.W., and Chase, G.C., 2006, Cenozoic exhumation of the northern Sierra Nevada, California, from (U–Th)/He thermochronology: Geological Society of America Bulletin, v. 118, p. 1481–1488.

Chapman, A.D., Saleeby, J.B., and Luffi, P.I., 2008, Rapid exhumation of the Rand schist: Corroborative evidence from garnet-based geospeedometry, thermochronology, and field studies: Geological Society of America Abstracts with Programs, v. 40, no. 1, Abstract 134709.

Church, H.V. Jr., and Krames, K.F., 1958, Correlation section: San Joaquin Valley, Riverdale thru Tejon Ranch Area (10 South): American Association of Petroleum Geologists, 3 miles to inch, 2 sheets.

Clark, M.K., and Farley, K.A., 2007, Sierra Nevada river incision from apatite ^{4}He/^{3}He thermochronometry [abs.]: EOS (Transactions, American Geophysical Union), v. 88, F2186.

Clark, M.K., Maheo, G., Saleeby, J., and Farley, K.A., 2005, The non-equilibrium (transient) landscape of the Sierra Nevada, California: GSA Today, v. 15, p. 4–10.

Clinton, J.F., Hauksson, E., and Solanki, K., 2006, An evaluation of the SCSN moment tensor solutions: Robustness of the Mw magnitude scale, style of faulting, and automation of the method: Bulletin of the Seismological Society of America, v. 96, p. 1689–1705.

Coles, S., Prothero, D.R., Quinn, J.P., and Swisher III, C.C., 1997, Magnetic stratigraphy of the middle Miocene Bopesta Formation, southern Sierra Nevada, California: *in* Girty, G.H., Hanson, R.E., and Cooper, J.D., eds., Geology of the western Cordilleran: Perspectives from undergraduate research. Los Angeles, California: Pacific Section Society of Economic Paleontologists and Mineralogists, v. 82, p. 21–34.

Cox, B.F., 1987, Stratigraphy, depositional environments, and paleotectonics of the Paleocene and Eocene Golar Formation, El Paso Mountains, California-geologic summary and roadlog: *in* Cox, B.F., ed., Basin analysis and paleontology of the Paleocne and Eocene Golar Formation, El Paso Mountains, California: Pacific Section, Society of Economic Paleontologists and Mineralogists Guidebook, v. 57, p. 1–29.

Dalrymple, G.B., 1963, Potassium-argon dates of some Cenozoic volcanic rocks of the Sierra Nevada, California: Geological Society of America Bulletin, v. 74 n. 4, p. 379–390.

Davis, G.H., and Green, J.H., 1962, Structural control of the interior drainage, southern San Joaquin Valley, California: United States Geological Survey Professional Paper 34 450D, p. D89–D91.

Davis, T.L., and Lagoe, M.B., 1988, A structural interpretation of major tectonic events affecting the western and southern margins of the San Joaquin Valley, California: Field Trip Guidebook – Pacific Section: Society of Economic Paleontologists and Mineralogists, v. 60, p. 65–87.

Davis, G.A., Monger, J.W.H., and Burchfiel, B.C., 1978, Mesozoic construction of the Cordilleran 'collage', central British Columbia to central California: *in* Howell, D.G., and McDougal, K.A., eds., Mesozoic Paleogeography of the western United States, Pacific Coast Paleogeography Symposium 2, Society of Economic Paleontologists and Mineralogists, p. 1–32.

Dibblee, T.W. Jr., and Louke, G.P., 1970, Geologic map of the Tehachapi quadrangle, Kern County, California: United States Geological Survey, Miscellaneous Geologic Investigations Map I-607, scale 1:62,500.

Dibblee, T.W. Jr., Bruer, W.G., Hackel, O., and Warne, A.H., 1965, Geologic map of the southeastern San Joaquin Valley (Kern River to Grapevine Canyon) Kern County, California: *in* Hackel, O., ed., Pacific Section, American Association of Petroleum Geologists Guidebook, California: Geology of southeastern San Joaquin Valley.

Dickinson, W.R., 1996, Kinematics of transrotational tectonism in the California Transverse Ranges and its contribution to cumulative slip along the San Andreas transform fault system: Geological Society of America Special Paper 305, 46 pp.

Diepenbroch, A., 1933, Mt. Poso Oil Field (Kern County): California Oil Fields, California Division of Oil and Gas, v. 19, no. 2, p. 5–33.

Dixon, T.H., Miller, M., Farina, F., Wang, H., and Johnson, D., 2000, Present-day motion of the Sierra Nevada block and some tectonic implications for the Basin and Range Province, North American Cordillera: Tectonics, v. 19, p. 1–24.

Dodge, F.C.W., Millard, H.T. Jr., and Elsheimer, H.N., 1982, Compositional variations and abundances of selected elements in granitoid rocks and constituent minerals, central Sierra Nevada batholith, California: United States Geological Survey Professional Paper 1248, 24 p.

Du Bray, E.A., and Dellinger, D.A., 1981, Geologic map of the Golden Trout Wilderness, southern Sierra Nevada, California, United States Geological Survey Miscellaneous Field Studies Map MF-1231-A.

Ducea, M., 2001, The California arc: Thick granitic batholiths, eclogitic residues, lithosphere scale thrusting, and magmatic flare-ups: GSA Today, no. 11, p. 4–10.

Ducea, M.N., and Saleeby, J.B., 1996, Buoyancy sources for a large, unrooted mountain range, the Sierra Nevada, California; evidence from xenolith thermobarometry: Journal of Geophysical Research, v. 101, p. 8229–8244.

Ducea, M.N., and Saleeby, J.B., 1998, The age and origin of a thick mafic-ultramafic keel from beneath the Sierra Nevada batholith: Contributions to Mineralogy and Petrology, v. 133, p. 169–185.

Dunne, G.C., and Walker, J.D., 2004, Structure and evolution of the east Sierran thrust system, east central California: Tectonics, v. 23, TC4012, doi:10.1029/2002TC001478.

Dunwoody, J.A., 1969, San Joaquin Valley Kingsburg to Tejon Hills, Pacific Section, American Association of Petroleum Geologists, Correlation Section, n. 17.

Dunwoody, J.A., 1986, Southern San Joaquin Valley from San Andreas fault to Sierra Nevada Foothills, American Association Petroleum Geologists, Correlation Section, n. 8.

Evernden, J.F., Savage, D.E., Gurnis, G.H., and James, G.T., 1964, Potassium-argon dates and the Cenozoic mammalian chronology of North America: American Journal of Science, v. 262, p. 1145–1980.

Farmer, G.L., Glazner, A.F., and Manley, C.R., 2002, Did lithosphere delamination trigger late Cenozoic potassic volcanism in the southern Sierra Nevada, California?: Geological Society of America Bulletin, v. 114, p. 754–768.

Fay, N.P., Bennett, R.A., and Hreinsdottir, S., 2008, Contemporary vertical velocity of the central Basin and Range and uplift of the southern Sierra Nevada: Geophysical Research Letters, v. 35, L20309, doi:10.1029/2008GL034949.

Fliedner, M.M., Klemperer, S.L., and Christensen, N.I., 2000, Three-dimensional seismic model of the Sierra Nevada arc, California, and its implications for crustal and upper mantle composition: Journal of Geophysical Research, v. 105, p. 10,899–10,921.

Furlong, K.P., and Schwartz, S.Y., 2004, Influence of the Mendocino Triple junction on the tectonics of coastal California: Annual Review of Earth and Planetary Science, v. 32, p. 403–433.

Gilbert, G.K., 1928, Studies of Basin and Range Structure: United States Geological Survey Professional Paper 153, 92 p.

Goodman, E.D., and Malin, P.E., 1992, Evolution of the southern San Joaquin Basin and mid-Tertiary transitional tectonics, central California: Tectonics, v. 11, p. 478–498.

Grove, K., 1993, Latest Cretaceous basin formation within the Salinian terrane of west-central California: Geological Society of America Bulletin, v. 105, p. 447–463.

Guacci, G., and Purcell, C.W., 1978, Evidence for middle Pleistocene and possible Holocene faulting on the Pond-Poso Creek fault, southern San Joaquin Valley, California: Geological Society of America Abstracts With Programs, v. 10, no. 3, p. 108.

Hackel, O., 1966, Summary of the geology of the Great Valley: *in* Bailey, E.H.G., ed., The Geology of Northern California, California Division of Mines and Geology, Bulletin 190, 217–238.

Hammond, W.C., and Thatcher, W., 2005, Northwest Basin and Range tectonic deformation observed with global positioning system: Journal of Geophysical Research, v. 110, B10405, doi:10.1029/2005JB003678.

Henry, C.D., and Perkins, M.E., 2001, Sierra Nevada-Basin and Range transition near Reno, Nevada: Two stage development at 12 and 3 Ma: Geology, v. 29, p. 719–722.

Hewlett, J.S., and Jordon, D.W., 1994, Stratigraphic and combination traps within a seismic sequence framework, Miocene Stevens turbitites, Bakersfield Arch, California: *in* Weimer, P., and Posamentier, H.W., eds., Siliciclastic sequence stratigraphy-Recent developments and applications: American Association of Petroleum Geologists Memoir 58, p. 135–162.

Hilton, G.S., McClelland, E.J., Klausing, R.L., and Kunkel, F., 1963, Geology, hydrology, and quality of water in the Terra Bella-Lost Hills area, San Joaquin Valley, California: United States Geological Survey Open File Report 63-47&48, 158 pp.

Hirst, B., 1986, Tectonic development of the Tejon and adjacent areas, Kern County, California, in Structure and stratigraphy of the east side San Joaquin Valley, Pacific Section, American Association of Petroleum Geologists Guidebook, Pat Bell ed., 2–8.

House, M.A., Wernicke, B.P., Farley, K.A., and Dumitru, T.A., 1997, Cenozoic thermal evolution of the central Sierra Navada, from (U–Th)/He Thermochronometry: Earth and Planetary Science Letters, v. 151, p. 167–179.

House, M.A., Wernicke, B.P., and Farley, K.A., 1998, Dating topography of the Sierra Nevada, California, using apatite (U–Th)/He ages: Nature, v. 396, p. 66–69.

House, M.A., Wernicke, B.P., and Farley, K.A., 2001, Paleo-geomorphology of the Sierra Nevada, California, from (U–Th)/He ages in apatite: America Journal of Science, v. 301, p. 77–102.

Huber, N.K., 1981, Amount and Timing of Late Cenozoic Uplift and Tilt of the Central Sierra Nevada, California – Evidence from the Upper San Joaquin River Basin: Geological Survey Professional Paper 1197, p. 1–28.

Huntington, K.W., Wernicke, B.P., and Eiler, J.M., 2009, The influence of climate change and uplift on Colorado Plateau paleotemperatures from carbonate 'clumped isotope' thermometry: Tectonics (in press).

Imperato, D.P., 1995, Studies of the stratigraphy and structure of the Great Valley of California and implications for plate tectonics [Ph.D. Dissertation]: University of California, Santa Barbara, 271 pp.

Ingersoll, R.V., 1978, Paleogeography and paleotectonics of the late Mesozoic forearc basin of northern and central California: *in* Howell, D., ed., Mesozoic Paleogeography of the Western United States: Pacific Section, Society of Economic Paleontologists and Mineralogists, p. 471–482.

Jayko, A.S., Blake, M.C. Jr., and Harms, T.A., 1987, Attenuation of the Coast Range ophiolite by extensional faulting and nature of the Coast Range 'thrust', California: Tectonics, v. 6, p. 475–488.

Jones, L.M., and Dollar, R.S., 1986, Evidence of basin-and-range extensional tectonics in the Sierra Nevada; the Durrwood Meadows swarm, Tulare County, California (1983–1984): Bulletin of the Seismological Society of America, v. 76, p. 439–461.

Jones, C.H., Kanamori, H., and Roeker, S.W., 1994, Missing roots and mantle 'drips': Regional Pn and teleseismic arrival times in the southern Sierra Nevada and vicinity, California: Journal of Geophysical Research, v. 99, p. 4567–4601.

Kistler, R.W., 1990, Two different lithosphere types in the Sierra Nevada, California: *in* Anderson, J.L., ed., The nature and origin of Cordilleran Magmatism, Geological Society of America Memoir 174, p. 271–282.

Klausing, R.L., and Lohman, K.E., 1964, Upper Pliocene marine strata on the east side of the San Joaquin Valley, California: United States Geological Survey Professional Paper 475-D, p. 14–17.

Kylander-Clark, A.R.C., Coleman, D.S., Glazner, A.F., and Bartley, J.M., 2005, Evidence for 65 km of dextral slip across Owens Valley, California, since 83 Ma: Geological Society of America Bulletin, v. 117, no. 7/8, p. 962–968; doi:10.1130/B25624.1.

Le Pourhiet, L., Gurnis, M., and Saleeby, J., 2006, Mantle instability beneath the Sierra Nevada Mountains in California and Death Valley extension: Earth and Planetary Science Letters, v. 251, p. 104–119.

Le, K., Lee, J., Owen, L.A., and Finkel, R., 2007, Late Quaternary slip rates along the Sierra Nevada frontal fault zone: Slip partitioning across the western margin of the eastern California shear zone-Basin and Range Province: Geological Society of America Bulletin, v. 119, p. 240–256.

Lingren, W., 1911, The Tertiary gravels of the Sierra Nevada of California: United States Geological Survey Professional Paper, 222 pp.

Lin, G., Shearer, P.M., and Hauksson, E., 2007, Applying a three-dimensional velocity model, waveform cross correlation, and cluster analysis to locate southern California seismicity from 1981 to 2005: Journal of Geophysical Research, v. 112, B12,309, 14 p.

Lofgren, B.E., and Klausing, R.L., 1969, Land subsidence due to ground-water withdrawal, Tulare-Wasco area, California: United States Geological Survey Professional Paper, 437-B, 103 p.

Loomis, D.P., and Burbank, D.W., 1988, The stratigraphic evolution of the El Paso Basin, Southern California; implications for the Miocene development of the Garlock Fault and uplift of the Sierra Nevada: Geological Society of America Bulletin, v. 100, p. 12–28.

Lucas, S.G., and Reynolds, R.E., 1991, Late Cretaceous (?) Plesiosaurs from Cajon Pass, California: San Bernardino County Museum Association Quarterly, v. 38, p. 53–54.

Luffi, P., Saleeby, J., Lee, C.T.A., and Ducea, M., 2009, Lithospheric mantle duplex beneath the central Mojave Desert revealed by xenoliths from Dish Hill, California: Journal of Geophysical Research, doi:10.1029/2008JB005906.

MacPherson, B.A., 1978, Sedimentation and trapping mechanism in upper Miocene Stevens and older turbidite fans of southeastern San Joaquin Valley, California: American Association Petroleum Geologists Bulletin, v. 62, p. 2243–2274.

Mahéo, G., Farley, K.A., Clark, M.K., and Shuster, D., 2004, Cooling and Exhumation of the Sierra Nevada Batholith in the Mount Whitney Area (California) Based on (U–Th)/He Thermochronometry: Eos (Transactions of the American Geophysical Union), v. 85, p. 1252.

Maheo, G., Saleeby, J., Saleeby, Z., and Farley, K.A., 2009, Tectonic control on southern Sierra Nevada topography, California: Tectonics (in press).

Malin, P.E., Goodman, E.D., Henyey, T.L., Li, Y-G., Okaya, D.A., and Saleeby, J.B., 1994, Significance of seismic reflections beneath a tilted exposure of deep continental crust, Tehachapi Mountains, California: Journal of Geophysical Research, v. 100, p. 2069–2087.

Miller, D.D., 1999, Sequence stratigraphy and controls on deposition of the upper Cenozoic Tulare Formation, San Joaquin Valley, unpublished [Ph.D. Dissertation]: California, Stanford University, 179 pp.

Monastero, F.C., Sabin, A.E., and Walker, J.D., 1997, Evidence for post-early Miocene initiation of movement on the Garlock Fault from offset of the Cudahy Camp Formation, east central California: Geology, v. 25, p. 247–250.

Monastero, F.C., Walker, J.D., Katzenstein, A.M., and Sabin, A.E., 2002, Neogene evolution of the Indian Wells Valley, east-central California: *in* Glazner, A.F., Walker, J.D., and Bartley, J.M., eds., Geologic Evolution of the Mojave Desert and Southwestern Basin and Range: Geological Society of America Memoir 195, p. 199–228.

Moxom, I.W., and Graham, S.A., 1987, History and controls of subsidence in the Late Cretaceous–Tertiary Great Valley forearc basin, California: Geology, v. 15, p. 626–629.

Nadin, E.S., 2007, Structure and history of the Kern Canyon fault system, southern Sierra Nevada, unpublished [Ph.D. Thesis]: California, California Institute of Technology, 297 pp.

Nadin, E.S., and Saleeby, J., 2008, Disruption of regional primary structure of the Sierra Nevada batholith, California: *in* Wright, J.E., and Shervais, J.W., eds., Ophiolites, arcs and batholiths: A tribute to Cliff Hopson. Geological Society of America Special Paper 438, p. 429–454.

Nadin, E.S., and Saleeby, J., 2009, Quaternary reactivation of the Kern Canyon fault system, southern Sierra Nevada, CA: Geological Society of America Bulletin (in press).

Namson, J.S., and Davis, T.L., 1988, Seismically active fold and thrust belt in the San Joaquin Valley, central California: Geological Society of America, v. 100, p. 257–273.

Nilsen, T.H., 1993, Stratigraphy of the Cretaceous Hornbrook Formation, southern Oregon and northern California: United States Geological Survey Professional Paper 1521, 89 pp.

Nilsen, T.H., Dibblee, T.W., and Addicott, W.O., 1973, Lower and Middle Tertiary Stratigraphic Units of the San Emigdio and Western Tehachapi Mountains, California: United States Geological Survey Bulletin 1372-H, p. H1–H23.

Nugent, L.E. Jr., 1942, The genesis of subordinate conjugate faulting in the Kern River salient (California): Journal of Geology, v. 50, p. 900–913.

Olson, H.C., 1988, Middle Tertiary stratigraphy, depositional environments, paleoecology, and tectonic history of the southeastern San Joaquin Basin, California: unpublished [Ph.D. Dissertation]: California, Stanford University, 353 pp.

Oskin, M., and Stock, J., 2003, Pacific–North America plate motion and opening of the Upper Delfin Basin, northern Gulf of California, Mexico: GSA Bulletin, vol. 115, p. 1173–1190.

Page, W., 2005, Assessment of seismic refraction survey at Lake Isabella Auxiliary Dam: Report to URS Corporation, Oakland, for the United States Army Corps of Engineers, Sacramento District, 27 September 2005.

Pickett, D.A., and Saleeby, J.B., 1993, Thermobarometry of Cretaceous rocks of the Tehachapi Mountains, California: Plutonism and metamorphism in deep levels of the Sierra Nevada batholith: Journal of Geophysical Research, v. 98, p. 609–629.

Poage, M.A., and Chamberlain, C.P., 2002, Stable isotope evidence for a pre-Basin and Range rain shadow in the western Basin and Range: Implications for the paleotopography of the Sierra Nevada: Tectonics, v. 21, p. 1034, doi:10.1029/2001TC001303.

Pysklywec, R.N., and Cruden, A.R., 2004, Coupled crust–mantle dynamics and intraplate tectonics; two-dimensional numerical and three-dimensional analogue modeling: Geochemistry, Geophysics, Geosystems – G^3, v. 748, p. 22.

Ransome, F.L., 1898, Some lava flows on the western slopes of the Sierra Nevada: American Journal of Science, v. 5, p. 355–375.

Reibe, C.S., Kirchner, J.W., Granger, D.E., and Finkel, R.C., 2000, Erosional equilibrium and disequilibrium in the Sierra Nevada, inferred from cosmogenic ^{26}Al and ^{10}Be in alluvial sediment: Geology, v. 28, p. 803–806.

Reid, S.A., 1988, Late Cretaceous and Paleogene sedimentation along the east side of the San Joaquin Basin: *in* Graham, S.A., ed., Studies of the Geology of the San Joaquin Basin. Pacific Section, Society of Economic Paleontologists and Mineralogists. v. 60, p. 157–171.

Repenning, C.A., 1960, Geologic summary of the central Valley of California with reference to the disposal of liquid radioactive waste: United States Geological Survey, Tace element Investigations Report 769, 69 pp.

Ross, D.C., 1986, Basement–rock correlations across the White Wolf–Breckenridge–southern Kern Canyon fault zone, southern Sierra Nevada, California: United States Geological Survey Bulletin, v. 1651, 25 pp.

Ross, D.C., 1989, The metamorphic and plutonic rocks of the southernmost Sierra Nevada, California and their tectonic framework: US Geological Survey Professional Paper 1381, 159 p.

Ruppert, S., Fliedner, M.M., and Zandt, G., 1998, Thin crust and active upper mantle beneath the southern Sierra Nevada in the western United States: Tectonophysics, v. 286, p. 237–252.

Saleeby, J.B., 1992, Petrotectonic and paleogeographic settings of US Cordilleran ophiolites: *in* Burchfiel, B.C., Lipman, P.W., and Zoback, M.L., eds., The Cordilleran Orogen: Conterminous US: Geological Society of America, The Geology of North America, v. G-3, p. 653–682.

Saleeby, J., 2003, Segmentation of the Laramide slab-evidence from the southern Sierra Nevada region: Geological Society of America Bulletin, v. 115, p. 655–668.

Saleeby, J., 2007, Western extent of the Sierra Nevada batholith in the Great Valley basement [abs.]: EOS (Transactions, American Geophysical Union), v. 88, F2186.

Saleeby, J., and Foster, Z., 2004, Topographic response to mantle lithosphere removal, southern Sierra Nevada region, California: Geology, v. 32, p. 245–248.

Saleeby, J., Ducea, M., and Clemens-Knott, D., 2003, Production and loss of high-density batholithic root, southern Sierra Nevada region: Tectonics, v. 22, p. 1–24, doi: 10.1029/2002TC001374.

Saleeby, J., Farley, K., Kistler, R.W., and Fleck, R., 2007, Thermal evolution and exhumation of deep level batholithic exposures, southernmost Sierra Nevada, California: *in* Cloos, M., Carlson, W.D., Gilbert, M.C., Liou, J.G., and Sorensen, S.S., eds., Geological Society of America Special Paper 419, Convergent Margin Terranes and Associated Regions, a Tribute to W.G. Ernst, Chap. 2, p. 39–66.

San Joaquin Nuclear Project, 1975, Early site review report: Los Angeles, Department of Water and Power, report submitted to the US Nuclear Regulatory Commission, 5 volumes.

Schemmann, K., Unruh, J.R., and Moores, E.M., 2007, Kinematics of Franciscan complex exhumation: New insights from the geology of Mount Diablo, California: Geological Society of America Bulletin, v. 120, 543–555.

Schott, R.C., and Johnson, C.M., 2001, Garnet-bearing trondhjemite and other conglomerate clasts from the Gualala basin, California: Sedimentary record of the missing western portion of the Salinian magmatic arc?: Geological Society of America Bulletinv. 1137, pp. 870–880.

Sella, G.F., Dixon, T.H., and Mao, A., 2002, REVEL: A model for recent plate velocities from space geodesy: Journal of Geophysical Research, v. 107, p. 17.

Smith, A.R., 1964, Geologic map of California, Bakersfield sheet: California Division of Mines and Geology, scale 1:250,000.

Stock, G.M., Anderson, R.S., and Finkel, R.C., 2004, Pace of landscape evolution in the Sierra Nevada, California, revealed by cosmogenic dating of cave sediments: Geology, v. 32 no. 3, p. 193–196, doi: 10.1130/G20197.1.

Stock, G.M., Anderson, R.S., and Finkel, R.C., 2005, Rates of erosion and topographic evolution of the Sierra Nevada, California, inferred from cosmogenic ^{26}Al and ^{10}Be concentrations: Earth Surface Processes and Landforms, v. 30, p. 985–1006.

Surpless, B.E., Stockli, D.F., Dumitru, T.A., and Miller, E.L., 2002, Two-phase westward encroachment of Basin and Range extension into the northern Sierra Nevada: Tectonics, v. 21, p. 1002, doi: 10.1029/2000TC001257.

Townley, S.D., and Allen, M.W., 1939, Descriptive catalogue of earthquakes of the Pacific Coast of the United States, 1769 to 1928: Bulletin of the Seismological Society of America, v. 29, p. 1–297.

Treasher, R.C., 1949, Kern County fault, Kern County, California: Geological Society of America Bulletin, v. 60, p. 1958.

Unruh, J.R., 1991, The uplift of the Sierra Nevada and implications for late Cenozoic epeirogeny in the western Cordillera: Geological Society of America Bulletin, v. 103, p. 1395–1404.

Unruh, J.R., and Hauksson, E., 2009, Seismotectonics of an evolving intracontinental plate boundary, southeastern California: Geological Society of America Special Paper (in press).

Unruh, J.R., Humphrey, J., and Barron, A., 2003, Transtensional model for the Sierra Nevada frontal fault system, eastern California: Geology, v. 31, p. 327–330.

Unruh, J.R., Dumitru, R.A., and Sawyer, T.L., 2007, Coupling of early Tertiary extension in the Great Valley forearc basin with blueschist exhumation in the underlying Franciscan accretionary wedge at Mount Diablo, California: Geological Society of America Bulletin, v. 119, p. 1347–1367.

Wakabayashi, J., and Sawyer, T.L., 2001, Stream incision, tectonics, uplift, and evolution of topography of the Sierra Nevada, California: Journal of Geology, v. 109, p. 539–562.

Webb, R.W., 1946, The geomorphology of the middle Kern River Basin, southern Sierra Nevada, California: Geological Society of America Bulletin, v. 57, p. 355–382.

Wentworth, C.M., Walter, A.W., Bartow, J.A., and Zoback, M.D., 1983, Evidence on the tectonic setting of the 1983 Coalinga earthquake from deep reflection and refraction profiles across the Kettlemen Hills, California: *in* Bennett, J.H., and Sherburne, R.W., eds., The 1983 Coalinga Earthquake: California Division of Mines and Geology Special Publication, v. 66, p. 293–306.

Wentworth, C.M., Fisher, G.R., Levine, P., and Jachens, R.C., 1995, The surface of crystalline basement, Great Valley and Sierra Nevada, California: A digital map database, United States Geological Survey Open-File Report, pp. 95–96.

Wernicke, B., and Snow, J.K., 1998, Cenozoic tectonism in the Basin and Range: Motion of the Sierran-Great Valley block: International Geology Review, v. 39, 111–118.

Wernicke, B., Axen, G.J., and Snow, J.K., 1988, Basin and Range extensional tectonics at the latitude of Las Vegas, Nevada: Geological Society of America Bulletin, v. 100, p. 1738–1757.

Wernicke, B., Clayton, R., Ducea, M.N., and Saleeby, J.B., 1996, Saleeby, and 16 others, 1996, Origins of high mountains on continents: The Southern Sierra Nevada: Science, v. 273, p. 190–193.

Wood, D.J., and Saleeby, J.B., 1998, Late Cretaceous–Paleocene extensional collapse and disaggregation of the southernmost Sierra Nevada batholith: International Geology Review, v. 39, p. 289–325.

Yan, Z., Clayton, R.W., and Saleeby, J., 2005, Seismic refraction evidence for steep faults cutting highly attenuated continental basement in the central Transverse Ranges, California: Geophysical Journal International, v. 160, p. 651–666.

Zandt, G., Gilbert, H., Owens, T., Ducea, M., Saleeby, J., and Jones, C., 2004, Active foundering of a continental arc root beneath the southern Sierra Nevada, California: Nature, v. 43, p. 41–45.